IMA Journal of Numerical Analysis (2019) **00**, 1–37
doi:10.1093/imanum/drz046

Linear second-order IMEX-type integrator for the (eddy current) Landau–Lifshitz–Gilbert equation

Giovanni Di Fratta, Carl-Martin Pfeiler, Dirk Praetorius, Michele Ruggeri and Bernhard Stiftner*
Institute for Analysis and Scientific Computing, TU Wien, Wiedner Hauptstrasse 8–10, 1040 Vienna, Austria
michele.ruggeri@asc.tuwien.ac.at *Corresponding author: bernhard.stiftner@asc.tuwien.ac.at

[Received on 30 November 2017; revised on 27 February 2019]

Combining ideas from Alouges *et al.* (2014, A convergent and precise finite element scheme for Landau–Lifschitz–Gilbert equation. *Numer. Math.*, **128**, 407–430) and Praetorius *et al.* (2018, Convergence of an implicit-explicit midpoint scheme for computational micromagnetics. *Comput. Math. Appl.*, **75**, 1719–1738) we propose a numerical algorithm for the integration of the nonlinear and time-dependent Landau–Lifshitz–Gilbert (LLG) equation, which is unconditionally convergent, formally (almost) second-order in time, and requires the solution of only one linear system per time step. Only the exchange contribution is integrated implicitly in time, while the lower-order contributions like the computationally expensive stray field are treated explicitly in time. Then we extend the scheme to the coupled system of the LLG equation with the eddy current approximation of Maxwell equations. Unlike existing schemes for this system, the new integrator is unconditionally convergent, (almost) second-order in time, and requires the solution of only two linear systems per time step.

Keywords: micromagnetism; finite elements; linear second-order time integration; implicit-explicit time-marching scheme; unconditional convergence

1. Introduction

1.1 *State of the art*

Nowadays, the study of magnetization processes in magnetic materials and the development of fast and reliable tools to perform large-scale micromagnetic simulations are the focus of considerable research as they play a fundamental role in the design of many technological devices. Applications to magnetic recording, in which the external field can change fast so that the hysteresis properties are not accurately described by a static approach, require accurate numerical methods to study the dynamics of the magnetization distribution. In this context a well-established model to describe the time evolution of the magnetization in ferromagnetic materials is the Landau–Lifshitz–Gilbert equation (LLG) introduced in Landau & Lifshitz (1935); Gilbert (1955).

Recently, the numerical integration of LLG has been the subject of many mathematical studies; see, e.g., the review articles Kružík & Prohl (2006); García-Cervera (2007); Cimrák (2008), the monograph Prohl (2001) and the references therein. The main challenges concern the strong nonlinearity of the problem, a nonconvex unit-length constraint, which forces the solutions to take their pointwise values in the unit sphere, an intrinsic energy law, which combines conservative and dissipative effects and

should be preserved by the numerical scheme, as well as the presence of nonlocal field contributions, which prescribe the (possibly nonlinear) coupling with other partial differential equations (PDEs). One important aspect of the research is related to the development of unconditionally convergent methods, for which the numerical analysis does not require imposing any Courant-Friedrichs-Lewy (CFL) condition on the relation of the spatial and temporal discretization parameters.

The seminal works Bartels & Prohl (2006); Alouges (2008) propose numerical time-marching schemes, based on lowest-order finite elements in space, which are proven to be unconditionally convergent towards a weak solution of LLG in the sense of Alouges & Soyeur (1992). The implicit midpoint scheme of Bartels & Prohl (2006) is formally of second order in time. It inherently preserves some of the fundamental properties of LLG, such as the pointwise constraint (at the nodes of the mesh) and the energy law. However, it requires the solution of a nonlinear system of equations per time step. The tangent plane scheme of Alouges (2008) is based on an equivalent reformulation of LLG, which gives rise to a variational formulation in the tangent space of the current magnetization state. It requires the solution of only one linear system per time step and employs the nodal projection at each time step to enforce the pointwise constraint at a discrete level. For an implicit–explicit approach for the full effective field we refer to Alouges *et al.* (2012); Bruckner *et al.* (2014). Moreover, extensions for the discretization of the coupling of LLG with the full Maxwell equations, the eddy current equation, a balance law for the linear momentum (magnetostriction) and a spin diffusion equation for the spin accumulation have been considered in Le & Tran (2013); Abert *et al.* (2014); Baňas *et al.* (2014, 2015); Le *et al.* (2015); Feischl & Tran (2017). Formally, the tangent plane scheme and its aforementioned extensions are of first order in time. The nodal projection step can be omitted and this leads to an additional consistency error, which is also first-order in time (Abert *et al.*, 2014). For this projection-free variant the recent work by Feischl & Tran (2017) derives rigorous *a priori* error estimates, which are of first order in time and space.

A tangent plane scheme with an improved convergence order in time is introduced and analyzed in Alouges *et al.* (2014). Like Alouges (2008) the proposed method is based on a predictor–corrector approach, which combines a linear reformulation of the equation with the use of the nodal projection for the numerical treatment of the pointwise constraint. However, the variational formulation for the linear update is designed in such a way that the scheme has a consistency error of order $2 - \varepsilon$ for any $0 < \varepsilon < 1$. For this reason this method is named an *(almost) second-order tangent plane scheme* in Alouges *et al.* (2014).

1.2 *Contributions of the present work*

In this work we propose a threefold extension of the improved tangent plane scheme from Alouges *et al.* (2014):

• During the design and the implementation of a micromagnetic code one of the main issues concerns the computation of the nonlocal magnetostatic interactions. In many situations, it turns out to be the most time-consuming part of micromagnetic simulations (Abert *et al.*, 2013). To cope with this problem we follow the approach by Praetorius *et al.* (2018) and propose an implicit–explicit treatment for the lower-order effective field contributions. Then only one expensive stray field computation per time step needs to be carried out. Nevertheless, our time stepping preserves the (almost) second-order convergence in time of the scheme, as well as the unconditional convergence result.

• The discovery of the giant magnetoresistance (GMR) effect in Baibich *et al.* (1988); Binasch *et al.* (1989) determined a breakthrough in magnetic hard disk storage capacity and encouraged several extensions of the micromagnetic model, which aim to describe the effect of spin-polarized currents on

magnetic materials. The most-used approaches involve extended forms of LLG, in which the classical energy-based effective field is augmented by additional terms in order to take into account the spin transfer torque effect; see Slonczewski (1996); Zhang & Li (2004); Thiaville *et al.* (2005). In this work we extend the abstract setting, the proposed algorithm and the convergence result so that the aforementioned extended forms of LLG are covered by our analysis.

• For the treatment of systems in which LLG is bidirectionally coupled with another time-dependent PDE, the works by Abert *et al.* (2014); Baňas *et al.* (2014, 2015); Le *et al.* (2015) propose integrators that completely decouple the time integration of LLG and the coupled equation. This treatment is very attractive in terms of computational cost and applicability of the scheme, since existing implementations, including solvers and preconditioning strategies for the building blocks of the system, can easily be reused. We show how such an approach can also be adopted for the improved tangent plane scheme. Combined with a second-order method for the coupled equation this leads to algorithms of global (almost) second order, for which the convergence result can be generalized. As an illustrative example, we analyze the coupling of LLG with eddy currents (ELLG), which is of relevant interest in several concrete applications (Bertotti *et al.*, 2002; Sun *et al.*, 2004; Hrkac *et al.*, 2005).

1.3 *Outline*

The remainder of this work is organized as follows. We conclude this section by recalling the notation used throughout the paper. In Sections 2 and in 3 we present the problem formulation and introduce the numerical algorithm. Then we state the convergence results for plain LLG and ELLG, respectively. In Section 4, for the convenience of the reader, we extend the formal argument by Alouges *et al.* (2014). In Sections 5 and 6 we prove the main results for plain LLG (Theorem 2.2) and ELLG (Theorem 3.2), respectively. Finally, Section 7 is devoted to numerical experiments.

1.4 *General notation*

Throughout this work we use the standard notation for Lebesgue, Sobolev and Bochner spaces and norms. For any domain U we denote the scalar product in $L^2(U)$ by $\langle\cdot,\cdot\rangle_U$ and the corresponding norm by $\|\cdot\|_U$. Vector-valued functions (as well as the corresponding function spaces) are indicated by bold letters. To abbreviate notation in proofs we write $A \lesssim B$ when $A \le cB$ for some generic constant $c > 0$, which is clear from the context and always independent of the discretization parameters. Moreover, $A \simeq B$ abbreviates $A \lesssim B \lesssim A$.

2. LLG equation

2.1 *LLG and weak solutions*

For a bounded Lipschitz domain $\omega \subset \mathbb{R}^3$ the Gilbert form of LLG reads

$$\partial_t \boldsymbol{m} = -\boldsymbol{m} \times \big(\boldsymbol{h}_{\mathrm{eff}}(\boldsymbol{m}) + \boldsymbol{\Pi}(\boldsymbol{m})\big) + \alpha\, \boldsymbol{m} \times \partial_t \boldsymbol{m} \qquad \text{in } \omega_T := (0,T) \times \omega, \tag{2.1a}$$

$$\partial_{\boldsymbol{n}} \boldsymbol{m} = \boldsymbol{0} \qquad \text{on } (0,T) \times \partial\omega, \tag{2.1b}$$

$$\boldsymbol{m}(0) = \boldsymbol{m}^0 \qquad \text{in } \omega, \tag{2.1c}$$

where $T > 0$ is the final time, $\alpha \in (0, 1]$ is the Gilbert damping constant and $\boldsymbol{m}^0 \in \boldsymbol{H}^1(\omega)$ is the initial data with $|\boldsymbol{m}^0| = 1$ a.e. in ω. The so-called effective field reads

$$\boldsymbol{h}_{\mathrm{eff}}(\boldsymbol{m}) = \ell_{\mathrm{ex}}^2 \Delta \boldsymbol{m} + \boldsymbol{\pi}(\boldsymbol{m}) + \boldsymbol{f}, \tag{2.1d}$$

where $\ell_{\mathrm{ex}} > 0$ is the exchange length, while the linear, self-adjoint and bounded operator $\boldsymbol{\pi} : \boldsymbol{L}^2(\omega) \to \boldsymbol{L}^2(\omega)$ collects the lower-order terms such as the stray field (for which $\boldsymbol{\pi}(\boldsymbol{m}) = -\nabla u$, where $u \in H^1(\mathbb{R}^3)$ solves (7.1)) and uniaxial anisotropy (see, e.g., (7.3)), and $\boldsymbol{f} \in C^1([0, T], \boldsymbol{L}^2(\omega))$ is the applied field. We note that

$$\boldsymbol{h}_{\mathrm{eff}}(\boldsymbol{m}) = -\frac{\delta \mathscr{E}_{\mathrm{LLG}}(\boldsymbol{m})}{\delta \boldsymbol{m}}, \text{ where } \mathscr{E}_{\mathrm{LLG}}(\boldsymbol{m}) = \frac{\ell_{\mathrm{ex}}^2}{2} \|\nabla \boldsymbol{m}\|_\omega^2 - \frac{1}{2} \langle \boldsymbol{\pi}(\boldsymbol{m}), \boldsymbol{m} \rangle_\omega - \langle \boldsymbol{f}, \boldsymbol{m} \rangle_\omega \tag{2.2}$$

is the micromagnetic energy functional. Further dissipative (e.g., spintronic) effects such as the Slonczewski contribution (Slonczewski, 1996) or the Zhang–Li contribution (Thiaville *et al.*, 2005; Zhang & Li, 2004) are collected in the (not necessarily linear) operator $\boldsymbol{\Pi} : \boldsymbol{H}^1(\omega) \cap \boldsymbol{L}^\infty(\omega) \to \boldsymbol{L}^2(\omega)$. For precise expressions we refer to (7.2) for the Slonczewski contribution and to (7.4) for the Zhang–Li contribution.

Note that solutions of LLG (2.1) formally satisfy $0 = \partial_t \boldsymbol{m} \cdot \boldsymbol{m} = \frac{1}{2} \partial_t |\boldsymbol{m}|^2$ and hence $|\boldsymbol{m}| = 1$ a.e. in ω_T. As in Alouges & Soyeur (1992) we use the following notion of weak solutions of (2.1):

Definition 2.1 With the foregoing notation a function $\boldsymbol{m} : \omega_T \to \mathbb{R}^3$ is called a weak solution of LLG (2.1) if the following properties (i)–(iv) are satisfied:

(i) $\boldsymbol{m} \in \boldsymbol{H}^1(\omega_T) \cap L^\infty(0, T; \boldsymbol{H}^1(\omega))$ with $|\boldsymbol{m}| = 1$ a.e. in ω_T;

(ii) $\boldsymbol{m}(0) = \boldsymbol{m}^0$ in the sense of traces;

(iii) for all $\boldsymbol{\varphi} \in \boldsymbol{H}^1(\omega_T)$,

$$\begin{aligned} \int_0^T \langle \partial_t \boldsymbol{m}, \boldsymbol{\varphi} \rangle_\omega \, \mathrm{d}t = \ell_{\mathrm{ex}}^2 \int_0^T \langle \boldsymbol{m} \times \nabla \boldsymbol{m}, \nabla \boldsymbol{\varphi} \rangle_\omega \, \mathrm{d}t - \int_0^T \langle \boldsymbol{m} \times \boldsymbol{f}, \boldsymbol{\varphi} \rangle_\omega \, \mathrm{d}t \\ - \int_0^T \langle \boldsymbol{m} \times \boldsymbol{\pi}(\boldsymbol{m}), \boldsymbol{\varphi} \rangle_\omega \, \mathrm{d}t - \int_0^T \langle \boldsymbol{m} \times \boldsymbol{\Pi}(\boldsymbol{m}), \boldsymbol{\varphi} \rangle_\omega \, \mathrm{d}t \\ + \alpha \int_0^T \langle \boldsymbol{m} \times \partial_t \boldsymbol{m}, \boldsymbol{\varphi} \rangle_\omega \, \mathrm{d}t; \end{aligned} \tag{2.3}$$

(iv) for almost all $\tau \in (0, T)$,

$$\mathscr{E}_{\mathrm{LLG}}(\boldsymbol{m}(\tau)) + \alpha \int_0^\tau \|\partial_t \boldsymbol{m}\|_\omega^2 \, \mathrm{d}t + \int_0^\tau \langle \partial_t \boldsymbol{f}, \boldsymbol{m} \rangle_\omega \, \mathrm{d}t - \int_0^\tau \langle \boldsymbol{\Pi}(\boldsymbol{m}), \partial_t \boldsymbol{m} \rangle_\omega \, \mathrm{d}t \le \mathscr{E}_{\mathrm{LLG}}(\boldsymbol{m}^0). \tag{2.4}$$

2.2 *Time discretization*

Let $N \in \mathbb{N}$ and $k := T/N$. Consider the uniform time steps $t_i := ik$ for $i = 0, \dots, N$ and the corresponding midpoints $t_{i+1/2} := (t_{i+1} + t_i)/2$. For a Banach space $\boldsymbol{B}$, e.g., $\boldsymbol{B} \in \{\boldsymbol{L}^2(\omega), \boldsymbol{H}^1(\omega)\}$, and a sequence $(\boldsymbol{\varphi}^i)_{i=-1}^N \in \boldsymbol{B}$, define the mean value and the discrete time derivative by

$$\boldsymbol{\varphi}^{i+1/2} := \frac{\boldsymbol{\varphi}^{i+1} + \boldsymbol{\varphi}^i}{2} \quad \text{and} \quad \mathrm{d}_t \boldsymbol{\varphi}^{i+1} := \frac{\boldsymbol{\varphi}^{i+1} - \boldsymbol{\varphi}^i}{k} \quad \text{for} \quad i = 0, \dots, N-1.$$

For $\boldsymbol{\Theta}^k \in \mathbb{R}^{N\times 3}$, define the two-step approach by

$$\boldsymbol{\varphi}^{i,\boldsymbol{\Theta}} := \boldsymbol{\Theta}_{i3}^k \boldsymbol{\varphi}^{i+1} + \boldsymbol{\Theta}_{i2}^k \boldsymbol{\varphi}^i + \boldsymbol{\Theta}_{i1}^k \boldsymbol{\varphi}^{i-1} \quad \text{for} \quad i = 0, \dots, N-1.$$

For $i = 0, \dots, N-1$ and $t \in [t_i, t_{i+1})$, define

$$\begin{aligned} &\boldsymbol{\varphi}_k^{=}(t) := \boldsymbol{\varphi}^{i-1}, \quad \boldsymbol{\varphi}_k^{-}(t) := \boldsymbol{\varphi}^{i}, \quad \boldsymbol{\varphi}_k^{+}(t) := \boldsymbol{\varphi}^{i+1}, \quad \overline{\boldsymbol{\varphi}}_k(t) := \boldsymbol{\varphi}^{i+1/2}, \\ &\boldsymbol{\varphi}_k^{\boldsymbol{\Theta}}(t) := \boldsymbol{\varphi}^{i,\boldsymbol{\Theta}} \quad \text{and} \quad \boldsymbol{\varphi}_k(t) := \boldsymbol{\varphi}^{i+1} \frac{t - t_i}{t_{i+1} - t_i} + \boldsymbol{\varphi}^i \frac{t_{i+1} - t}{t_{i+1} - t_i}. \end{aligned} \tag{2.5}$$

Note that $\boldsymbol{\varphi}_k^{=}, \boldsymbol{\varphi}_k^{-}, \boldsymbol{\varphi}_k^{+}, \overline{\boldsymbol{\varphi}}_k, \boldsymbol{\varphi}_k^{\boldsymbol{\Theta}} \in L^2(0,T;\boldsymbol{B})$ and $\boldsymbol{\varphi}_k \in H^1(0,T;\boldsymbol{B})$ with $\partial_t \boldsymbol{\varphi}_k(t) = \mathrm{d}_t \boldsymbol{\varphi}^{i+1}$ for $t \in (t_i, t_{i+1})$.

2.3 *Space discretization*

Let $\mathscr{T}_h$ be a conforming triangulation of ω into compact tetrahedra $K \in \mathscr{T}_h$. We assume that $\mathscr{T}_h$ is κ-quasi-uniform, i.e., there exists $\kappa \geq 1$ such that the global mesh size $h > 0$ satisfies

$$\kappa^{-1} h \leq |K|^{1/3} \leq \operatorname{diam}(K) \leq \kappa h \quad \text{for all } K \in \mathscr{T}_h. \tag{2.6}$$

We suppose that $\mathscr{T}_h$ is weakly acute, i.e., the dihedral angles of all elements are smaller than or equal to $\pi/2$. We denote the space of $\mathscr{T}_h$-piecewise affine and globally continuous functions by

$$\boldsymbol{V}_h := (V_h)^3 \subset \boldsymbol{H}^1(\omega) \quad \text{with} \quad V_h := \{v_h \in C(\omega) : v_h|_K \in \mathscr{P}^1(K) \text{ for all } K \in \mathscr{T}_h\}.$$

Let $\mathscr{N}_h$ be the set of nodes of $\mathscr{T}_h$. Recall that $|\boldsymbol{m}| = 1$ and $\boldsymbol{m} \cdot \partial_t \boldsymbol{m} = 0$. To mimic the latter properties, we define the set of discrete admissible magnetizations on ω by

$$\mathscr{M}_h := \{\boldsymbol{\psi}_h \in \boldsymbol{V}_h : |\boldsymbol{\psi}_h(z_h)| = 1 \text{ for all } z_h \in \mathscr{N}_h\}$$

as well as the discrete tangent space

$$\mathscr{K}_h(\boldsymbol{\psi}_h) := \{\boldsymbol{\varphi}_h \in \boldsymbol{V}_h : \boldsymbol{\psi}_h(z_h) \cdot \boldsymbol{\varphi}_h(z_h) = 0 \text{ for all } z_h \in \mathscr{N}_h\} \quad \text{for all } \boldsymbol{\psi}_h \in \mathscr{M}_h.$$

2.4 *Almost second-order tangent plane scheme*

In this section we formulate our numerical integrator. For each time step t_i it approximates $\boldsymbol{m}(t_i)$ by $\boldsymbol{m}_h^i \in \mathscr{M}_h$ and $\partial_t \boldsymbol{m}(t_i)$ by $\boldsymbol{v}_h^i \in \mathscr{K}_h(\boldsymbol{m}_h^i)$. In some cases the evaluation of $\boldsymbol{\pi}(\boldsymbol{m}_h^i)$ and $\boldsymbol{\Pi}(\boldsymbol{m}_h^i)$ requires the solution of coupled PDEs (see, e.g., (7.1) for the stray field). Then the practical formulation of the overall integrator involves discretizations $\boldsymbol{\pi}_h(\boldsymbol{m}_h^i)$ and $\boldsymbol{\Pi}_h(\boldsymbol{m}_h^i)$ (e.g., by FEM or FEM-BEM coupling). Therefore, we consider the (computable) operators

$$\boldsymbol{\pi}_h, \boldsymbol{\Pi}_h : \mathscr{M}_h \to \boldsymbol{L}^2(\omega) \quad \text{and} \quad \boldsymbol{\pi}_h^i, \boldsymbol{\Pi}_h^i : \boldsymbol{V}_h \times \mathscr{M}_h \times \mathscr{M}_h \to \boldsymbol{L}^2(\omega)$$

such that $\boldsymbol{\pi}_h(\boldsymbol{m}_h^i) \approx \boldsymbol{\pi}(\boldsymbol{m}_h^i)$, $\boldsymbol{\Pi}_h(\boldsymbol{m}_h^i) \approx \boldsymbol{\Pi}(\boldsymbol{m}_h^i)$, $\boldsymbol{\pi}_h^i(\boldsymbol{v}_h^i; \boldsymbol{m}_h^i, \boldsymbol{m}_h^{i-1}) \approx \boldsymbol{\pi}(\boldsymbol{m}_h^{i+1/2})$ and $\boldsymbol{\Pi}_h^i(\boldsymbol{v}_h^i; \boldsymbol{m}_h^i, \boldsymbol{m}_h^{i-1}) \approx \boldsymbol{\Pi}(\boldsymbol{m}_h^{i+1/2})$. We suppose that the operators $\boldsymbol{\pi}_h^i$ and $\boldsymbol{\Pi}_h^i$ are affine in $\boldsymbol{v}_h^i$. For concrete examples and further precise assumptions on those operators we refer to Remark 2.1 and Section 2.5. We extend the construction in (2.5) to the operator sequences $(\boldsymbol{\pi}_h^i)_{i=0}^{N-1}$ and $(\boldsymbol{\Pi}_h^i)_{i=0}^{N-1}$ via

$$\boldsymbol{\pi}_{hk}^-(t) := \boldsymbol{\pi}_h^i \quad \text{and} \quad \boldsymbol{\Pi}_{hk}^-(t) := \boldsymbol{\Pi}_h^i \quad \text{for all } t \in [t_i, t_{i+1}).$$

Finally, we require two stabilizations $M : \mathbb{R}_{>0} \to \mathbb{R}_{>0}$ and $\rho : \mathbb{R}_{>0} \to \mathbb{R}_{>0}$ such that

$$\lim_{k\to 0} M(k) = \infty \quad \text{with} \quad \lim_{k\to 0} M(k)k = 0, \tag{2.7a}$$

$$\lim_{k\to 0} \rho(k) = 0 \quad \text{with} \quad \lim_{k\to 0} k^{-1}\rho(k) = \infty. \tag{2.7b}$$

The canonical choices are

$$\rho(k) := |k \log k| \quad \text{and} \quad M(k) := |k \log k|^{-1}. \tag{2.7c}$$

We proceed as in Alouges *et al.* (2014, p. 415) and define the weight function

$$W_{M(k)}(s) := \begin{cases} \alpha + \dfrac{k}{2} \min\{s, M(k)\} & \text{for } s \geq 0, \\ \dfrac{2\alpha^2}{2\alpha + k \min\{-s, M(k)\}} & \text{for } s < 0. \end{cases} \tag{2.8}$$

With these preparations our numerical integrator reads as follows:

ALGORITHM 2.2 (Implicit–explicit tangent plane scheme)
Input: Approximation $\boldsymbol{m}_h^{-1} := \boldsymbol{m}_h^0 \in \mathscr{M}_h$ of initial magnetization.
Loop: For $i = 0, \dots, N-1$, iterate the following steps (a)–(c):
(a) Compute the discrete function

$$\lambda_h^i := -\ell_{\mathrm{ex}}^2 \, |\nabla \boldsymbol{m}_h^i|^2 + \big(\boldsymbol{f}(t_i) + \boldsymbol{\pi}_h(\boldsymbol{m}_h^i) + \boldsymbol{\Pi}_h(\boldsymbol{m}_h^i)\big) \cdot \boldsymbol{m}_h^i. \tag{2.9}$$

(b) Find $\boldsymbol{v}_h^i \in \mathscr{K}_h(\boldsymbol{m}_h^i)$ such that, for all $\boldsymbol{\varphi}_h \in \mathscr{K}_h(\boldsymbol{m}_h^i)$,

$$\begin{aligned} &\langle W_{M(k)}(\lambda_h^i)\, \boldsymbol{v}_h^i, \boldsymbol{\varphi}_h \rangle_\omega + \langle \boldsymbol{m}_h^i \times \boldsymbol{v}_h^i, \boldsymbol{\varphi}_h \rangle_\omega + \frac{\ell_{\mathrm{ex}}^2}{2}\, k\,(1+\rho(k))\, \langle \nabla \boldsymbol{v}_h^i, \nabla \boldsymbol{\varphi}_h \rangle_\omega \\ &= -\ell_{\mathrm{ex}}^2\, \langle \nabla \boldsymbol{m}_h^i, \nabla \boldsymbol{\varphi}_h \rangle_\omega + \langle \boldsymbol{f}(t_{i+1/2}), \boldsymbol{\varphi}_h \rangle_\omega + \langle \boldsymbol{\pi}_h^i(\boldsymbol{v}_h^i; \boldsymbol{m}_h^i, \boldsymbol{m}_h^{i-1}), \boldsymbol{\varphi}_h \rangle_\omega \\ &\quad + \langle \boldsymbol{\Pi}_h^i(\boldsymbol{v}_h^i; \boldsymbol{m}_h^i, \boldsymbol{m}_h^{i-1}), \boldsymbol{\varphi}_h \rangle_\omega . \end{aligned} \tag{2.10}$$

(c) Define $\boldsymbol{m}_h^{i+1} \in \mathscr{M}_h$ by

$$\boldsymbol{m}_h^{i+1}(z_h) := \frac{\boldsymbol{m}_h^i(z_h) + k\boldsymbol{v}_h^i(z_h)}{|\boldsymbol{m}_h^i(z_h) + k\boldsymbol{v}_h^i(z_h)|} \quad \text{for all } z_h \in \mathscr{N}_h. \tag{2.11}$$

Output: Approximations $\boldsymbol{m}_h^i \approx \boldsymbol{m}(t_i)$ for all $i = 0, \dots, N$.

REMARK 2.1 (i) Theorem 2.2 states the well-posedness of Algorithm 2.2 as well as unconditional convergence towards a weak solution of LLG in the sense of Definition 2.1.

(ii) The variational formulation (2.10) gives rise to a linear system for $\boldsymbol{v}_h^i$. However, in particular for stray field computations, the part of the resulting system matrix corresponding to the $\boldsymbol{\pi}_h^i$-contribution may be fully populated (or not explicitly available for hybrid FEM-BEM methods; Fredkin & Koehler, 1990). We refer to (iii)–(iv) below for two possible approaches to deal with this issue, which do not impair the formal convergence order of the scheme.

(iii) The chain rule gives rise to an operator $\boldsymbol{D}(\boldsymbol{m}, \partial_t \boldsymbol{m}) := \partial_t[\boldsymbol{\Pi}(\boldsymbol{m})]$, which is linear in the second argument. Suppose that $\boldsymbol{D}_h$ is a discretization of $\boldsymbol{D}$. The seminal work by Alouges *et al.* (2014) proposes

$$\boldsymbol{\pi}_h^i(\boldsymbol{v}_h^i; \boldsymbol{m}_h^i, \boldsymbol{m}_h^{i-1}) := \boldsymbol{\pi}_h(\boldsymbol{m}_h^i) + \frac{k}{2}\, \boldsymbol{\pi}_h(\boldsymbol{v}_h^i), \tag{2.12a}$$

$$\boldsymbol{\Pi}_h^i(\boldsymbol{v}_h^i; \boldsymbol{m}_h^i, \boldsymbol{m}_h^{i-1}) := \boldsymbol{\Pi}_h(\boldsymbol{m}_h^i) + \frac{k}{2}\, \boldsymbol{D}_h(\boldsymbol{m}_h^i, \boldsymbol{v}_h^i); \tag{2.12b}$$

see Proposition 4.1(i). The resulting linear system can then be solved with the convergent fixed-point iteration (5.1) described in the proof of Theorem 2.2(i).

(iv) Unlike Alouges *et al.* (2014) we propose to employ

$$\boldsymbol{\pi}_h^i(\boldsymbol{v}_h^i; \boldsymbol{m}_h^i, \boldsymbol{m}_h^{i-1}) := \begin{cases} \boldsymbol{\pi}_h(\boldsymbol{m}_h^0) & \text{for } i = 0, \\ \frac{3}{2}\, \boldsymbol{\pi}_h(\boldsymbol{m}_h^i) - \frac{1}{2}\, \boldsymbol{\pi}_h(\boldsymbol{m}_h^{i-1}) & \text{for } i \geq 1, \end{cases} \tag{2.13a}$$

$$\boldsymbol{\Pi}_h^i(\boldsymbol{v}_h^i;\boldsymbol{m}_h^i,\boldsymbol{m}_h^{i-1}) := \begin{cases} \boldsymbol{\Pi}_h(\boldsymbol{m}_h^0) & \text{for } i=0,\\ \boldsymbol{\Pi}_h(\boldsymbol{m}_h^i) + \frac{1}{2}\boldsymbol{D}_h(\boldsymbol{m}_h^i,\boldsymbol{m}_h^i) - \frac{1}{2}\boldsymbol{D}_h(\boldsymbol{m}_h^i,\boldsymbol{m}_h^{i-1}) & \text{for } i\geq 1; \end{cases} \tag{2.13b}$$

see Proposition 4.1(ii). In this way, the right-hand side of (2.10) is independent of $\boldsymbol{v}_h^i$. We note that our choice for the first time step ($i = 0$) corresponds to one step of the explicit Euler method for the lower-order terms. Hence, the first step leads to a second-order consistency error in the approximation of $\boldsymbol{m}$. The successive time steps ($i \geq 1$) correspond to steps of the explicit Adams–Bashforth two-step method for the lower-order terms. Any of these steps thus leads to a third-order consistency error in the approximation of $\boldsymbol{m}$ (and there are $\mathcal{O}(k^{-1})$ of such steps). Overall, one may thus expect a formal global second-order convergence of the scheme. This hypothesis is numerically confirmed in Section 7.1. In particular, for the first time step, any higher accuracy than that guaranteed by the explicit Euler method does not improve the formal convergence order of the scheme.

(v) The choice of ρ in (2.7c) leads to formally (almost) second-order-in-time convergence of Algorithm 2.2. In principle, it suffices to choose a sufficiently large constant $M(k) \equiv M > 0$; for details see Proposition 4.1.

(vi) Unlike the stabilized scheme, we note that the nonstabilized scheme $\rho(k) \equiv 0$ requires a CFL condition $k = \mathbf{o}(h)$ for the convergence proof; see also Remark 5.1.

2.5 *Main theorem for LLG integration*

To formulate the main result, which generalizes Alouges *et al.* (2014, Theorem 2), we require the following assumptions:

- Let $\mathscr{T}_h$ satisfy the assumptions of Section 2.3.
- Let $\boldsymbol{m}_h^0 \in \mathscr{M}_h$ satisfy

$$\boldsymbol{m}_h^0 \rightharpoonup \boldsymbol{m}^0 \quad \text{in } \boldsymbol{H}^1(\omega) \quad \text{as } h \to 0. \tag{2.14}$$

- For all $i \in \{0,\dots,N-1\}$, let $\boldsymbol{\pi}_h^i$ satisfy, for all $\boldsymbol{\psi}_h, \widetilde{\boldsymbol{\psi}}_h \in \boldsymbol{V}_h$ and all $\boldsymbol{\varphi}_h, \widetilde{\boldsymbol{\varphi}}_h \in \mathscr{M}_h$, the Lipschitz-type continuity

$$\|\boldsymbol{\pi}_h^i(\boldsymbol{\psi}_h;\boldsymbol{\varphi}_h,\widetilde{\boldsymbol{\varphi}}_h) - \boldsymbol{\pi}_h^i(\widetilde{\boldsymbol{\psi}}_h;\boldsymbol{\varphi}_h,\widetilde{\boldsymbol{\varphi}}_h)\|_\omega \leq C_{\boldsymbol{\pi}}\, k\, \|\boldsymbol{\psi}_h - \widetilde{\boldsymbol{\psi}}_h\|_\omega \tag{2.15a}$$

and the stability-type estimate

$$\|\boldsymbol{\pi}_h^i(\boldsymbol{\psi}_h;\boldsymbol{\varphi}_h,\widetilde{\boldsymbol{\varphi}}_h)\|_\omega \leq C_{\boldsymbol{\pi}}\, \big(k\, \|\boldsymbol{\psi}_h\|_\omega + \|\boldsymbol{\varphi}_h\|_\omega + \|\widetilde{\boldsymbol{\varphi}}_h\|_\omega\big). \tag{2.15b}$$

Moreover, for all sequences $\boldsymbol{\psi}_{hk}$ in $L^2(0,T;\boldsymbol{V}_h)$ and $\boldsymbol{\varphi}_{hk}$, $\widetilde{\boldsymbol{\varphi}}_{hk}$ in $L^2(0,T;\mathscr{M}_h)$ with $\boldsymbol{\psi}_{hk} \rightharpoonup \boldsymbol{\psi}$ and $\boldsymbol{\varphi}_{hk}, \widetilde{\boldsymbol{\varphi}}_{hk} \to \boldsymbol{\varphi}$ in $\boldsymbol{L}^2(\omega_T)$, we suppose consistency,

$$\boldsymbol{\pi}_{hk}^-(\boldsymbol{\psi}_{hk};\boldsymbol{\varphi}_{hk},\widetilde{\boldsymbol{\varphi}}_{hk}) \rightharpoonup \boldsymbol{\pi}(\boldsymbol{\varphi}) \quad \text{in } \boldsymbol{L}^2(\omega_T) \quad \text{as } h,k \to 0. \tag{2.15c}$$

- For all $i \in \{0,\dots,N-1\}$, let $\boldsymbol{\Pi}_h^i$ satisfy, for all $\boldsymbol{\psi}_h, \widetilde{\boldsymbol{\psi}}_h \in \boldsymbol{V}_h$ and all $\boldsymbol{\varphi}_h, \widetilde{\boldsymbol{\varphi}}_h \in \mathscr{M}_h$, the Lipschitz-type continuity

$$\|\boldsymbol{\Pi}_h^i(\boldsymbol{\psi}_h;\boldsymbol{\varphi}_h,\widetilde{\boldsymbol{\varphi}}_h) - \boldsymbol{\Pi}_h^i(\widetilde{\boldsymbol{\psi}}_h;\boldsymbol{\varphi}_h,\widetilde{\boldsymbol{\varphi}}_h)\|_\omega \leq C_{\boldsymbol{\Pi}}\, k\, \|\boldsymbol{\psi}_h - \widetilde{\boldsymbol{\psi}}_h\|_{\boldsymbol{H}^1(\omega)} \tag{2.16a}$$

and the stability-type estimate

$$\langle \boldsymbol{\Pi}_h^i(\boldsymbol{\psi}_h;\boldsymbol{\varphi}_h,\widetilde{\boldsymbol{\varphi}}_h), \boldsymbol{\psi}_h\rangle_\omega \leq C_{\boldsymbol{\Pi}}\, \|\boldsymbol{\psi}_h\|_\omega \big(k\, \|\boldsymbol{\psi}_h\|_{\boldsymbol{H}^1(\omega)} + \|\boldsymbol{\varphi}_h\|_{\boldsymbol{H}^1(\omega)} + \|\widetilde{\boldsymbol{\varphi}}_h\|_{\boldsymbol{H}^1(\omega)}\big). \tag{2.16b}$$

Moreover, for all sequences $\boldsymbol{\psi}_{hk}$ in $L^2(0,T;\boldsymbol{V}_h)$ and $\boldsymbol{\varphi}_{hk}$, $\widetilde{\boldsymbol{\varphi}}_{hk}$ in $L^2(0,T;\mathscr{M}_h)$ with $\boldsymbol{\psi}_{hk} \rightharpoonup \boldsymbol{\psi}$ and $\boldsymbol{\varphi}_{hk}, \widetilde{\boldsymbol{\varphi}}_{hk} \to \boldsymbol{\varphi}$ in $\boldsymbol{L}^2(\omega_T)$, we suppose consistency,

$$\boldsymbol{\Pi}_{hk}^{-}(\boldsymbol{\psi}_{hk};\boldsymbol{\varphi}_{hk},\widetilde{\boldsymbol{\varphi}}_{hk}) \rightharpoonup \boldsymbol{\Pi}(\boldsymbol{\varphi}) \quad \text{in } \boldsymbol{L}^2(\omega_T) \quad \text{as } h,k \to 0. \tag{2.16c}$$

THEOREM 2.2 (i) If the Lipschitz-type estimates (2.15a) and (2.16a) are satisfied, then there exists $k_0 > 0$ such that for all $0 < k < k_0$ the discrete variational formulation (2.10) admits a unique solution $\boldsymbol{v}_h^i \in \mathscr{K}_h(\boldsymbol{m}_h^i)$. In particular, Algorithm 2.2 is well defined.

(ii) Suppose that all preceding assumptions (2.14)–(2.16) are satisfied. Let $\boldsymbol{m}_{hk}$ be the postprocessed output (2.5) of Algorithm 2.2. Then there exists $\boldsymbol{m} \in \boldsymbol{H}^1(\omega_T) \cap L^\infty(0,T;\boldsymbol{H}^1(\omega))$, which satisfies Definition 2.1(i)–(iii), and a subsequence of $\boldsymbol{m}_{hk}$ converges weakly in $\boldsymbol{H}^1(\omega_T)$ towards $\boldsymbol{m}$ as $h,k \to 0$.

(iii) Under the assumptions of (ii) suppose that the convergence properties (2.14) as well as (2.15c) and (2.16c) hold with strong convergence. Moreover, suppose additionally that $\boldsymbol{f} \in C^1([0,T],\boldsymbol{L}^2(\omega)) \cap C([0,T],\boldsymbol{L}^3(\omega))$ and that $\boldsymbol{\pi}$ is $\boldsymbol{L}^3$-stable, i.e.,

$$\|\boldsymbol{\pi}(\boldsymbol{\varphi})\|_{\boldsymbol{L}^3(\omega)} \le C_{\boldsymbol{\pi}}' \, \|\boldsymbol{\varphi}\|_{\boldsymbol{L}^3(\omega)} \quad \text{for all } \boldsymbol{\varphi} \in \boldsymbol{H}^1(\omega). \tag{2.17}$$

Then, $\boldsymbol{m}$ from (ii) is a weak solution of LLG in the sense of Definition 2.1(i)–(iv).

REMARK 2.2 (i) If the solution $\boldsymbol{m} \in \boldsymbol{H}^1(\omega_T) \cap L^\infty(0,T;\boldsymbol{H}^1(\omega))$ of Definition 2.1 is unique, then the full sequence $\boldsymbol{m}_{hk}$ converges weakly in $\boldsymbol{H}^1(\omega_T)$ towards $\boldsymbol{m}$.

(ii) The assumptions (2.15) on $\boldsymbol{\pi}_h$ (even with strong convergence) as well as (2.17) on $\boldsymbol{\pi}$ are satisfied, e.g., for uniaxial anisotropy (see (7.3) below) and the stray field (see (7.1) below). Possible stray field discretizations include hybrid FEM-BEM approaches (Fredkin & Koehler, 1990); see Bruckner *et al.* (2014); Praetorius *et al.* (2018).

(iii) The Lipschitz-type estimates (2.15a) and (2.16a) are only used to prove that Algorithm 2.2 is well defined for sufficiently small $k > 0$. The stability estimates (2.15b) and (2.16b) are then used to prove some discrete energy estimate (Lemma 6.1). Finally, the consistency assumptions (2.15c) and (2.16c) are used to show that the existing limit satisfies the variational formulation of Definition 2.1(iii).

(iv) The assumptions on $\boldsymbol{\pi}_h$ and $\boldsymbol{\Pi}_h$ from (2.15)–(2.16) are only exploited for $\boldsymbol{\varphi}_h = \boldsymbol{m}_h^i$, $\widetilde{\boldsymbol{\varphi}}_h = \boldsymbol{m}_h^{i-1}$, and $\boldsymbol{\varphi}_{hk} = \boldsymbol{m}_{hk}^{-}$, $\widetilde{\boldsymbol{\varphi}}_{hk} = \boldsymbol{m}_{hk}^{=}$, $\boldsymbol{\psi}_{hk} = \boldsymbol{v}_{hk}^{-}$. Moreover, only (2.15a) and (2.16a) require general $\boldsymbol{\psi}_h, \widetilde{\boldsymbol{\psi}}_h$, while (2.15b) and (2.16b) are only exploited for $\boldsymbol{\psi}_h = \boldsymbol{v}_h^i$.

The proof of Theorem 2.2 is postponed to Section 5. Unique solvability of (2.10) will be proved with the Banach fixed-point theorem. Theorem 2.2(ii)–(iii) will be proved through an energy argument, which consists of the following three steps:

- bound the discrete energy (Lemma 5.1);
- extract weakly convergent subsequences having a common limit (Lemma 5.2);
- verify that this limit is a weak solution in the sense of Definition 2.1.

3. LLG equation with eddy currents

3.1 *ELLG and weak solutions*

Let $\Omega \subset \mathbb{R}^3$ be a bounded Lipschitz domain with $\Omega \supseteq \omega$ which represents a conducting body with its ferromagnetic part ω. ELLG reads

$$\partial_t \boldsymbol{m} = -\boldsymbol{m} \times \big(\boldsymbol{h}_{\mathrm{eff}}(\boldsymbol{m}) + \boldsymbol{\Pi}(\boldsymbol{m}) + \boldsymbol{h}\big) + \alpha\, \boldsymbol{m} \times \partial_t \boldsymbol{m} \qquad \text{in } \omega_T := (0,T) \times \omega, \tag{3.1a}$$

$$-\mu_0\,\partial_t \boldsymbol{m} = \mu_0\,\partial_t \boldsymbol{h} + \nabla \times (\sigma^{-1}\nabla \times \boldsymbol{h}) \qquad \text{in } \Omega_T := (0,T)\times\Omega, \tag{3.1b}$$

$$\partial_{\mathbf{n}}\boldsymbol{m} = \mathbf{0} \qquad \text{on } (0,T)\times\partial\omega, \tag{3.1c}$$

$$(\nabla \times \boldsymbol{h}) \times \mathbf{n} = \mathbf{0} \qquad \text{on } (0,T)\times\partial\Omega, \tag{3.1d}$$

$$(\boldsymbol{m},\boldsymbol{h})(0) = (\boldsymbol{m}^0,\boldsymbol{h}^0) \qquad \text{in } \omega\times\Omega. \tag{3.1e}$$

Here, $\sigma \in L^\infty(\Omega)$ with $\sigma \geq \sigma_0 > 0$ is the conductivity of Ω, and $\mu_0 > 0$ is the vacuum permeability. The initial condition $\boldsymbol{h}^0 \in \boldsymbol{H}(\mathbf{curl};\Omega)$ satisfies the compatibility conditions

$$\nabla\cdot(\boldsymbol{h}^0 + \chi_\omega \boldsymbol{m}^0) = 0 \text{ in } \Omega \quad \text{and} \quad (\boldsymbol{h}^0 + \chi_\omega \boldsymbol{m}^0)\cdot\mathbf{n} = 0 \text{ on } \partial\Omega. \tag{3.2}$$

Unlike Le & Tran (2013, Definition 2.1) we define the energy functional

$$\mathscr{E}_{\mathrm{ELLG}}(\boldsymbol{m},\boldsymbol{h}) := \frac{\ell_{\mathrm{ex}}^2}{2}\|\nabla\boldsymbol{m}\|_\omega^2 - \frac{1}{2}\langle\boldsymbol{\pi}(\boldsymbol{m}),\boldsymbol{m}\rangle_\omega - \langle\boldsymbol{f},\boldsymbol{m}\rangle_\omega + \frac{1}{2}\|\boldsymbol{h}\|_\Omega^2.$$

As in Alouges & Soyeur (1992); Le & Tran (2013), we use the following notion of weak solutions of ELLG (3.1):

Definition 3.1 With the foregoing notation the pair $(\boldsymbol{m},\boldsymbol{h})$ is called a weak solution of ELLG (3.1) if the following conditions 3.1–3.1 are satisfied:

(i) $\boldsymbol{m} \in \boldsymbol{H}^1(\omega_T) \cap L^\infty(0,T;\boldsymbol{H}^1(\omega))$ with $|\boldsymbol{m}| = 1$ a.e. in ω_T;

(ii) $\boldsymbol{h} \in H^1(0,T;\boldsymbol{L}^2(\Omega)) \cap L^\infty(0,T;\boldsymbol{H}(\mathrm{curl};\Omega))$;

(iii) $\boldsymbol{m}(0) = \boldsymbol{m}^0$ and $\boldsymbol{h}(0) = \boldsymbol{h}^0$ in the sense of traces;

(iv) for all $\boldsymbol{\varphi} \in \boldsymbol{H}^1(\omega_T)$ and for all $\boldsymbol{\zeta} \in L^2(0,T;\boldsymbol{H}(\mathrm{curl},\Omega))$,

$$\begin{aligned}\int_0^T \langle\partial_t\boldsymbol{m},\boldsymbol{\varphi}\rangle_\omega\,\mathrm{d}t = \ell_{\mathrm{ex}}^2\int_0^T \langle\boldsymbol{m}\times\nabla\boldsymbol{m},\nabla\boldsymbol{\varphi}\rangle_\omega\,\mathrm{d}t - \int_0^T \langle\boldsymbol{m}\times\boldsymbol{f},\boldsymbol{\varphi}\rangle_\omega\,\mathrm{d}t \\ - \int_0^T \langle\boldsymbol{m}\times\boldsymbol{\pi}(\boldsymbol{m}),\boldsymbol{\varphi}\rangle_\omega\,\mathrm{d}t - \int_0^T \langle\boldsymbol{m}\times\boldsymbol{\Pi}(\boldsymbol{m}),\boldsymbol{\varphi}\rangle_\omega\,\mathrm{d}t \\ - \int_0^T \langle\boldsymbol{m}\times\boldsymbol{h},\boldsymbol{\varphi}\rangle_\omega\,\mathrm{d}t + \alpha\int_0^T \langle\boldsymbol{m}\times\partial_t\boldsymbol{m},\boldsymbol{\varphi}\rangle_\omega\,\mathrm{d}t,\end{aligned} \tag{3.3a}$$

$$-\mu_0\int_0^T \langle\partial_t\boldsymbol{m},\boldsymbol{\zeta}\rangle_\omega\,\mathrm{d}t = \mu_0\int_0^T \langle\partial_t\boldsymbol{h},\boldsymbol{\zeta}\rangle_\Omega\,\mathrm{d}t + \int_0^T \langle\sigma^{-1}\nabla\times\boldsymbol{h},\nabla\times\boldsymbol{\zeta}\rangle_\Omega\,\mathrm{d}t; \tag{3.3b}$$

(v) for almost all $\tau \in (0,T)$,

$$\begin{aligned}\mathscr{E}_{\mathrm{ELLG}}(\boldsymbol{m}(\tau),\boldsymbol{h}(\tau)) + \alpha\int_0^\tau \|\partial_t\boldsymbol{m}\|_\omega^2\,\mathrm{d}t + \int_0^\tau \langle\partial_t\boldsymbol{f},\boldsymbol{m}\rangle_\omega\,\mathrm{d}t \\ + \frac{1}{\mu_0}\int_0^\tau \|\sigma^{-1/2}\nabla\times\boldsymbol{h}\|_\Omega^2\,\mathrm{d}t - \int_0^\tau \langle\boldsymbol{\Pi}(\boldsymbol{m}),\partial_t\boldsymbol{m}\rangle_\omega\,\mathrm{d}t \leq \mathscr{E}_{\mathrm{ELLG}}(\boldsymbol{m}^0,\boldsymbol{h}^0).\end{aligned} \tag{3.4}$$

3.2 *Discretization*

We adopt the notation of Section 2.2. Let $\mathscr{T}_h$ be a conforming triangulation of Ω into compact tetrahedra $K \in \mathscr{T}_h$. Suppose that $\mathscr{T}_h$ is κ-quasi-uniform (see (2.6)). Let $\mathscr{T}_h|_\omega := \{K \in \mathscr{T}_h : K \subset \overline{\omega}\}$, and suppose that $\overline{\omega} = \bigcup \{K \in \mathscr{T}_h|_\omega\}$. Let $\mathscr{N}_h$ (resp. $\mathscr{N}_h|_\omega$) be the set of nodes of $\mathscr{T}_h$ (resp. $\mathscr{T}_h|_\omega$). We suppose that $\mathscr{T}_h|_\omega$ is weakly acute and define $\boldsymbol{V}_h$, $\mathscr{M}_h$ and $\mathscr{K}_h(\cdot)$ with respect to $\mathscr{T}_h|_\omega$ as in Section 2.3. Finally, the space of Nédélec edge elements of second type (Nédélec, 1986) on Ω reads

$$\mathscr{X}_h := \{\boldsymbol{\zeta}_h \in \boldsymbol{H}(\mathbf{curl}; \Omega) : \boldsymbol{\zeta}_h|_K \in \mathscr{P}^1(K) \text{ for all } K \in \mathscr{T}_h\} \subset \boldsymbol{H}(\mathbf{curl}; \Omega).$$

3.3 *Almost second-order tangent plane scheme*

In this section we extend Algorithm 2.2 to ELLG (3.1). More precisely we combine Algorithm 2.2 for the LLG-part with an implicit midpoint scheme for the eddy current part.

ALGORITHM 3.2 (Decoupled ELLG algorithm)
Input: $\boldsymbol{\Theta}^k \in \mathbb{R}^{N\times 3}$, approximations $\boldsymbol{m}_h^{-1} := \boldsymbol{m}_h^0 \in \mathscr{M}_h$ and $\boldsymbol{h}_h^{-1} := \boldsymbol{h}_h^0 \in \mathscr{X}_h$ of the initial values.
Loop: For $i = 0, \dots, N-1$ iterate the following steps (a)–(d):
(a) Compute the discrete function

$$\lambda_h^i := -\ell_{\mathrm{ex}}^2 |\nabla \boldsymbol{m}_h^i|^2 + \big(\boldsymbol{f}(t_i) + \boldsymbol{\pi}_h(\boldsymbol{m}_h^i) + \boldsymbol{\Pi}_h(\boldsymbol{m}_h^i) + \boldsymbol{h}_h^i\big) \cdot \boldsymbol{m}_h^i.$$

(b) Find $\boldsymbol{v}_h^i \in \mathscr{K}_h(\boldsymbol{m}_h^i)$ such that, for all $\boldsymbol{\varphi}_h \in \mathscr{K}_h(\boldsymbol{m}_h^i)$,

$$\begin{aligned}
&\langle W_M(\lambda_h^i)\boldsymbol{v}_h^i, \boldsymbol{\varphi}_h\rangle_\omega + \langle \boldsymbol{m}_h^i \times \boldsymbol{v}_h^i, \boldsymbol{\varphi}_h\rangle_\omega + \frac{\ell_{\mathrm{ex}}^2}{2} k\,(1+\rho(k))\,\langle \nabla \boldsymbol{v}_h^i, \nabla \boldsymbol{\varphi}_h\rangle_\omega \\
&= -\ell_{\mathrm{ex}}^2 \langle \nabla \boldsymbol{m}_h^i, \nabla \boldsymbol{\varphi}_h\rangle_\omega + \langle \boldsymbol{f}(t_{i+1/2}), \boldsymbol{\varphi}_h\rangle_\omega + \langle \boldsymbol{\pi}_h^i(\boldsymbol{v}_h^i; \boldsymbol{m}_h^i, \boldsymbol{m}_h^{i-1}), \boldsymbol{\varphi}_h\rangle_\omega \\
&\quad + \langle \boldsymbol{\Pi}_h^i(\boldsymbol{v}_h^i; \boldsymbol{m}_h^i, \boldsymbol{m}_h^{i-1}), \boldsymbol{\varphi}_h\rangle_\omega + \langle \boldsymbol{h}_h^{i,\boldsymbol{\Theta}}, \boldsymbol{\varphi}_h\rangle_\omega.
\end{aligned} \tag{3.5a}$$

(c) Define $\boldsymbol{m}_h^{i+1} \in \mathscr{M}_h$ by

$$\boldsymbol{m}_h^{i+1}(z_h) := \frac{\boldsymbol{m}_h^i(z_h) + k\boldsymbol{v}_h^i(z_h)}{|\boldsymbol{m}_h^i(z_h) + k\boldsymbol{v}_h^i(z_h)|} \quad \text{for all } z_h \in \mathscr{N}_h.$$

(d) Find $\boldsymbol{h}_h^{i+1} \in \mathscr{X}_h$ such that, for all $\boldsymbol{\zeta}_h \in \mathscr{X}_h$, it holds that,

$$-\mu_0 \langle \mathrm{d}_t \boldsymbol{m}_h^{i+1}, \boldsymbol{\zeta}_h\rangle_\omega = \mu_0 \langle \mathrm{d}_t \boldsymbol{h}_h^{i+1}, \boldsymbol{\zeta}_h\rangle_\Omega + \langle \sigma^{-1}\nabla \times \boldsymbol{h}_h^{i+1/2}, \nabla \times \boldsymbol{\zeta}_h\rangle_\Omega. \tag{3.5b}$$

Output: Approximations $\boldsymbol{m}_h^i \approx \boldsymbol{m}(t_i)$ and $\boldsymbol{h}_h^i \approx \boldsymbol{h}(t_i)$ for all $i = 0, \dots, N$.

REMARK 3.1 (i) Theorem 3.2 states the well-posedness of Algorithm 3.2, as well as unconditional convergence towards a weak solution of ELLG in the sense of Definition 3.1.

(ii) It depends on the choice of $\boldsymbol{\pi}_h^i$, $\boldsymbol{\Pi}_h^i$ and $\boldsymbol{\Theta}^k$ (the latter determining $\boldsymbol{h}_h^{i,\boldsymbol{\Theta}}$ in (3.5a)) whether steps (b)–(d) of Algorithm 3.2 have to be solved simultaneously or sequentially and whether the resulting systems of equations are linear or nonlinear; see (iii)–(v) below for three possible choices.

(iii) Combining the approach of Alouges *et al.* (2014) for $\boldsymbol{\pi}_h^i$ and $\boldsymbol{\Pi}_h^i$ (see (2.12)) with the choice $\boldsymbol{\Theta}_{i1}^k = 0$ and $\boldsymbol{\Theta}_{i2}^k := 1/2 =: \boldsymbol{\Theta}_{i3}^k$ for all $i = 0, \dots, N-1$, i.e.,

$$\boldsymbol{h}_h^{i,\boldsymbol{\Theta}} := \boldsymbol{h}_h^{i+1/2} = \boldsymbol{h}_h^i + \frac{k}{2}\,\mathrm{d}_t\,\boldsymbol{h}_h^{i+1}, \tag{3.6}$$

steps (b)–(d) of Algorithm 3.2 have to be solved simultaneously. Moreover, because of step (c), the overall system is nonlinear in $\boldsymbol{v}_h^i$. The proof of Theorem 3.2(i) provides a convergent fixed-point solver (6.1).

(iv) Following our approach for plain LLG, we propose to employ (2.13) for $\boldsymbol{\pi}_h^i$ and $\boldsymbol{\Pi}_h^i$. For $\boldsymbol{\Theta}^k$ we propose to use $\boldsymbol{\Theta}_{01}^k = 0$, $\boldsymbol{\Theta}_{02}^k := 1$, $\boldsymbol{\Theta}_{03}^k := 0$ for the first time step ($i = 0$) and $\boldsymbol{\Theta}_{i1}^k = -1/2$, $\boldsymbol{\Theta}_{i2}^k := 3/2$, $\boldsymbol{\Theta}_{i3}^k := 0$ for all $i = 1, \dots, N-1$, i.e.,

$$\boldsymbol{h}_h^{i,\boldsymbol{\Theta}} := \begin{cases} \boldsymbol{h}_h^i & \text{for } i = 0, \\ \frac{3}{2}\,\boldsymbol{h}_h^i - \frac{1}{2}\,\boldsymbol{h}_h^{i-1} & \text{for } i \geq 1. \end{cases}$$

The first time step corresponds to one step of the explicit Euler method, while we use an explicit Adams–Bashforth two-step method for all successive steps. Two main advantages of this approach are that the numerical integrator decouples the time stepping for LLG and the eddy current equation (so that steps (b)–(d) of Algorithm 3.2 can be solved sequentially) and that only two linear systems need to be solved in each time step. For this approach and the one described in (iii), choosing ρ according to (2.7c), Algorithm 3.2 is formally of almost second order in time, as numerically confirmed in Section 7.3.

(v) Another approach leading to a fully linear algorithm can be obtained by using (2.13) for $\boldsymbol{\pi}_h^i$ and $\boldsymbol{\Pi}_h^i$, (3.6) for $\boldsymbol{h}_h^{i,\boldsymbol{\Theta}}$ and replacing $\langle \mathrm{d}_t\,\boldsymbol{m}_h^{i+1}, \boldsymbol{\zeta}_h \rangle_\omega$ in the left-hand side of (3.5b) by $\langle \boldsymbol{v}_h^i, \boldsymbol{\zeta}_h \rangle_\omega$. Then steps (b) and (d) of Algorithm 3.2 have to be solved simultaneously and consist in solving a linear system for $\boldsymbol{v}_h^i$ and $\boldsymbol{h}_h^{i+1/2}$. However, Lemma 4.1 predicts that $\partial_t \boldsymbol{m} = \boldsymbol{v} + \mathcal{O}(k)$, and thus we only expect first-order convergence in time. This fact is confirmed numerically in Section 7.3.

(vi) In practice we solve (3.5b) for the unknown $\boldsymbol{v}_h := \boldsymbol{h}_h^{i+1/2} \in \mathcal{X}_h$, i.e., we compute the unique $\boldsymbol{v}_h \in \mathcal{X}_h$ such that, for all $\boldsymbol{\zeta}_h \in \mathcal{X}_h$,

$$\frac{2\mu_0}{k}\langle \boldsymbol{v}_h, \boldsymbol{\zeta}_h \rangle_\Omega + \langle \sigma^{-1} \nabla \times \boldsymbol{v}_h, \nabla \times \boldsymbol{\zeta}_h \rangle_\Omega = -\mu_0 \langle \mathrm{d}_t\,\boldsymbol{m}_h^{i+1}, \boldsymbol{\zeta}_h \rangle_\omega + \frac{2\mu_0}{k}\langle \boldsymbol{h}_h^i, \boldsymbol{\zeta}_h \rangle_\Omega.$$

Then, $\boldsymbol{h}_h^{i+1} := 2\,\boldsymbol{v}_h - \boldsymbol{h}_h^i$ solves (3.5b).

3.4 *Main theorem for ELLG integration*

This section states our convergence result for Algorithm 3.2. In Le *et al.* (2015), Le & Tran (2013) and Baňas *et al.* (2015), similar results are proved for a first-order tangent plane scheme for ELLG and for the Maxwell-LLG system, respectively.

THEOREM 3.2 (i) Suppose that the Lipschitz-type estimates (2.15a) and (2.16a) are satisfied. Suppose that the coupling parameter $\boldsymbol{\Theta}^k \in \mathbb{R}^{N\times 3}$ satisfies

$$\max_{ij} |\boldsymbol{\Theta}^k_{ij}| \le C_{\boldsymbol{\Theta}} < \infty \quad \text{and} \quad \sum_{j=1}^{3} \boldsymbol{\Theta}^k_{ij} = 1 \quad \text{for all } i \in \{0,\dots,N-1\}. \tag{3.7}$$

Then there exists $k_0 > 0$ such that for all $0 < k < k_0$ the discrete variational formulation (3.5) admits a unique solution $(\boldsymbol{v}_h^i, \boldsymbol{h}_h^{i+1}) \in \mathscr{K}_h(\boldsymbol{m}_h^i) \times \mathscr{X}_h$. In particular, Algorithm 3.2 is well defined.

(ii) Suppose that (3.7) as well as all assumptions from Section 2.5, is satisfied. Let $(\boldsymbol{m}_{hk}, \boldsymbol{h}_{hk})$ be the postprocessed output (2.5) of Algorithm 3.2. Then there exist $\boldsymbol{m} \in \boldsymbol{H}^1(\omega_T) \cap L^\infty(0,T;\boldsymbol{H}^1(\omega))$ and $\boldsymbol{h} \in H^1(0,T;\boldsymbol{L}^2(\Omega)) \cap L^\infty(0,T;\boldsymbol{H}(\mathrm{curl},\Omega))$, which satisfy Definition 3.1(i)–(iv), and a subsequence of $(\boldsymbol{m}_{hk}, \boldsymbol{h}_{hk})$ converges weakly in $\boldsymbol{H}^1(\omega_T) \times \boldsymbol{L}^2(\Omega_T)$ towards $(\boldsymbol{m},\boldsymbol{h})$ as $h,k \to 0$.

(iii) Under the assumptions of (ii) suppose that the convergence properties (2.14), as well as (2.15c) and (2.16c), hold with strong convergence. Moreover, suppose additionally that $\boldsymbol{f} \in C^1([0,T],\boldsymbol{L}^2(\omega)) \cap C([0,T],\boldsymbol{L}^3(\omega))$ and that $\boldsymbol{\pi}$ is $\boldsymbol{L}^3$-stable (2.17). Finally, let the CFL condition $k = \mathbf{o}(h^{3/2})$ be satisfied. Then the pair $(\boldsymbol{m},\boldsymbol{h})$ from (ii) is a weak solution of ELLG in the sense of Definition 3.1(i)–(v).

REMARK 3.2 (i) If the solution $(\boldsymbol{m},\boldsymbol{h})$ of Definition 3.1 is unique, then the full sequence $(\boldsymbol{m}_{hk}, \boldsymbol{h}_{hk})$ converges weakly in $\boldsymbol{H}^1(\omega_T) \times \boldsymbol{L}^2(\Omega_T)$ towards $(\boldsymbol{m},\boldsymbol{h})$.

(ii) We stress that the CFL condition $k = \mathbf{o}(h^{3/2})$ is only required to prove the energy law (3.4). Even without the CFL condition, Algorithm 3.2 is stable, and Theorem 3.2(ii) guarantees convergence to a weak solution $(\boldsymbol{m},\boldsymbol{h})$ with bounded energy, which satisfies the variational form (3.3) of ELLG.

(iii) If the strong CFL condition $k = \mathbf{o}(h^2)$ is satisfied (i.e., even stronger than in Theorem 3.2(iii)) then Theorem 3.2(ii) holds also for vanishing stabilization $\rho(k) \equiv 0$.

(iv) The compatibility condition (3.2) of the initial data is not exploited in the proof of Theorem 3.2. In particular, the discrete initial data do not have to satisfy any 'discrete compatibility condition'.

(v) If $\langle \mathrm{d}_t \boldsymbol{m}_h^{i+1}, \boldsymbol{\zeta}_h \rangle_\omega$ in (3.5b) is replaced by $\langle \boldsymbol{v}_h^i, \boldsymbol{\zeta}_h \rangle_\omega$ then Theorem 3.2(iii) holds without the CFL condition $k = \mathbf{o}(h^{3/2})$, which is only exploited in (6.13) below. However, as mentioned in Remark 3.1(v), the overall integrator then appears to be of first order in time.

The proof of Theorem 3.2 is postponed to Section 6. For the LLG part of ELLG (3.1) we follow our proof of Theorem 2.2. For the eddy current part we adapt the techniques of Le & Tran (2013); Baňas *et al.* (2015); Le *et al.* (2015); Praetorius *et al.* (2018) to the setting of Algorithm 3.2.

4. Derivation of second-order tangent plane scheme

In this section we adapt Alouges *et al.* (2014); Praetorius *et al.* (2018) in order to motivate Algorithm 2.2 and to underpin that it is of (almost) second order in time. Since solutions $\boldsymbol{m}$ to LLG satisfy $\boldsymbol{m} \cdot \partial_t \boldsymbol{m} = 0$ a.e. in ω, we define, for any $\boldsymbol{\psi} \in \boldsymbol{C}^\infty(\overline{\omega})$ with $|\boldsymbol{\psi}| = 1$, its tangent space

$$\mathscr{K}(\boldsymbol{\psi}) := \big\{\boldsymbol{\varphi} \in \boldsymbol{C}^\infty(\overline{\omega}) : \boldsymbol{\psi} \cdot \boldsymbol{\varphi} = 0 \text{ in } \omega\big\},$$

as well as the pointwise projection onto $\mathscr{K}(\boldsymbol{\psi})$ by

$$\mathbb{P}_{\boldsymbol{\psi}}(\boldsymbol{u}) := \boldsymbol{u} - (\boldsymbol{u}\cdot\boldsymbol{\psi})\boldsymbol{\psi} \quad \text{for all } \boldsymbol{u} \in \boldsymbol{C}^\infty(\overline{\omega}).$$

LEMMA 4.1 (Alouges *et al.*, 2014, p. 413). For $\boldsymbol{m} \in \boldsymbol{C}^\infty\left(\overline{\omega_T}\right)$ with $|\boldsymbol{m}| = 1$,

$$\frac{\boldsymbol{m}(t) + k\boldsymbol{v}(t)}{|\boldsymbol{m}(t) + k\boldsymbol{v}(t)|} = \boldsymbol{m}(t+k) + \mathscr{O}(k^3), \quad \text{where} \quad \boldsymbol{v}(t) := \partial_t \boldsymbol{m}(t) + \frac{k}{2}\,\mathbb{P}_{\boldsymbol{m}(t)}(\partial_{tt}\boldsymbol{m}(t)) \tag{4.1}$$

for all $t \in [0, T-k]$.

Recall the stabilizations $M(\cdot)$ and $\rho(\cdot)$ from (2.7), as well as the weight function $W_{M(k)}(\cdot)$ from (2.8). The following lemma is implicitly found in Alouges *et al.* (2014, p. 415). With (2.7a) it proves, in particular, that $W_{M(k)}(\cdot) \geq \alpha/2$ if $k > 0$ is sufficiently small. The proof follows from the Taylor theorem and is included in the extended preprint Di Fratta *et al.* (2017).

LEMMA 4.2 (Di Fratta *et al.*, 2017, Lemma 12). The weight function $W_{M(k)}(\cdot)$ satisfies the following two assertions:
(i) $|W_{M(k)}(s) - \alpha| \leq \frac{M(k)k}{2}$ for all $s \in \mathbb{R}$. (ii) If $M(k) \geq B > 0$ and $k < k_0 := \alpha/B$, then

$$\left|\alpha + \frac{k}{2}s - W_{M(k)}(s)\right| \leqslant \frac{B^2}{2\alpha}\,k^2 \quad \text{for all } s \in [-B, B].$$

The following proposition shows that the consistency error of Algorithm 2.2 is $\mathscr{O}(k^2 + k\rho(k))$. For $\boldsymbol{\Pi} = \boldsymbol{0}$ and $\boldsymbol{f}$ constant in time (4.4a) is implicitly contained in Alouges *et al.* (2014, Section 6), while (4.4b) adapts some further ideas from Praetorius *et al.* (2018). The proof extends Alouges *et al.* (2014, Section 6) to our setting and is given in Di Fratta *et al.* (2017).

PROPOSITION 4.1 (Di Fratta *et al.*, 2017, Proposition 13). Let $\boldsymbol{D}(\cdot,\cdot)$ be obtained from the formal operator $\boldsymbol{D}(\boldsymbol{m}(t), \partial_t \boldsymbol{m}(t)) := \partial_t[\boldsymbol{\Pi}(\boldsymbol{m}(t))]$ and the chain rule. For $\boldsymbol{\psi} \in \boldsymbol{C}^\infty(\overline{\omega})$ and $\boldsymbol{w}, \boldsymbol{\varphi} \in \boldsymbol{H}^1(\omega)$ and with $\lambda(\boldsymbol{\psi}) := \big(\boldsymbol{h}_{\mathrm{eff}}(\boldsymbol{\psi}) + \boldsymbol{\Pi}(\boldsymbol{\psi})\big) \cdot \boldsymbol{\psi}$ define the bilinear form

$$\mathbf{b}(\boldsymbol{\psi}; \boldsymbol{w}, \boldsymbol{\varphi}) := \langle W_{M(k)}\big(\lambda(\boldsymbol{\psi})\big)\boldsymbol{w}, \boldsymbol{\varphi}\rangle_\omega + \langle \boldsymbol{\psi} \times \boldsymbol{w}, \boldsymbol{\varphi}\rangle_\omega + \frac{\ell_{\mathrm{ex}}^2}{2}\,k\,(1 + \rho(k))\,\langle \nabla \boldsymbol{w}, \nabla \boldsymbol{\varphi}\rangle_\omega. \tag{4.2}$$

Let $\boldsymbol{m} \in \boldsymbol{C}^\infty\left(\overline{\omega_T}\right)$ be a strong solution of LLG (2.1), which satisfies

$$B := \|\lambda(\boldsymbol{m})\|_{L^\infty(\omega_T)} \leq M(k) < \infty. \tag{4.3}$$

Then $\boldsymbol{v}$ from (4.1) satisfies the following two assertions:
(i) For $t \in [0, T-k]$ there exists $\boldsymbol{R}_1 = \mathscr{O}(k^2 + k\rho(k))$ such that, for all $\boldsymbol{\varphi} \in \mathscr{K}(\boldsymbol{m})$,

$$\begin{aligned} &\mathbf{b}(\boldsymbol{m}; \boldsymbol{v}(t), \boldsymbol{\varphi}) - \frac{k}{2}\,\langle \boldsymbol{\pi}(\boldsymbol{v}(t)), \boldsymbol{\varphi}\rangle_\omega - \frac{k}{2}\,\langle \boldsymbol{D}(\boldsymbol{m}(t), \boldsymbol{v}(t)), \boldsymbol{\varphi}\rangle_\omega \\ &\quad = -\ell_{\mathrm{ex}}^2 \langle \nabla \boldsymbol{m}(t), \nabla \boldsymbol{\varphi}\rangle_\omega + \langle \boldsymbol{f}\big(t + k/2\big), \boldsymbol{\varphi}\rangle_\omega + \langle \boldsymbol{\pi}(\boldsymbol{m}(t)), \boldsymbol{\varphi}\rangle_\omega \\ &\qquad + \langle \boldsymbol{\Pi}(\boldsymbol{m}(t)), \boldsymbol{\varphi}\rangle_\omega + \langle \boldsymbol{R}_1, \boldsymbol{\varphi}\rangle_\omega. \end{aligned} \tag{4.4a}$$

(ii) For $t \in [k, T-k]$ there exists $\boldsymbol{R}_2 = \mathcal{O}(k^2 + k\rho(k))$ such that, for all $\boldsymbol{\varphi} \in \mathcal{K}(\boldsymbol{m})$,

$$\begin{aligned}\mathbf{b}(\boldsymbol{m}; \boldsymbol{v}(t), \boldsymbol{\varphi}) = -\ell_{\mathrm{ex}}^2 \langle \nabla \boldsymbol{m}(t), \nabla \boldsymbol{\varphi} \rangle_\omega + \langle \boldsymbol{f}\big(t + k/2\big), \boldsymbol{\varphi} \rangle_\omega + \frac{3}{2} \langle \boldsymbol{\pi}(\boldsymbol{m}(t)), \boldsymbol{\varphi} \rangle_\omega \\ - \frac{1}{2} \langle \boldsymbol{\pi}(\boldsymbol{m}(t-k)), \boldsymbol{\varphi} \rangle_\omega + \langle \boldsymbol{\Pi}(\boldsymbol{m}(t)), \boldsymbol{\varphi} \rangle_\omega + \frac{1}{2} \langle \boldsymbol{D}(\boldsymbol{m}(t), \boldsymbol{m}(t)), \boldsymbol{\varphi} \rangle_\omega \\ - \frac{1}{2} \langle \boldsymbol{D}(\boldsymbol{m}(t), \boldsymbol{m}(t-k)), \boldsymbol{\varphi} \rangle_\omega + \langle \boldsymbol{R}_2, \boldsymbol{\varphi} \rangle_\omega. \end{aligned} \tag{4.4b}$$

Moreover, it holds that $\lambda(\boldsymbol{m}) = -\ell_{\mathrm{ex}}^2 |\nabla \boldsymbol{m}|^2 + \big(\boldsymbol{f} + \boldsymbol{\pi}(\boldsymbol{m}) + \boldsymbol{\Pi}(\boldsymbol{m})\big) \cdot \boldsymbol{m}$.

REMARK 4.2 (i) For $\rho(k) = \mathcal{O}(k)$, Proposition 4.1 yields $\boldsymbol{R}_1, \boldsymbol{R}_2 = \mathcal{O}(k^2)$ and therefore second-order accuracy of the consistency error. In this case, however, the convergence result of Theorem 2.2 requires the CFL condition $k = \mathbf{o}(h)$. Instead, the choice $\rho(k) := k|\log(k)|$ requires no CFL condition and leads to $\rho(k) = \mathcal{O}(k^{1-\varepsilon})$ and hence to $\boldsymbol{R}_1, \boldsymbol{R}_2 = \mathcal{O}(k^{2-\varepsilon})$ for any $\varepsilon > 0$. For details we refer to Remark 5.1 below.

(ii) In Proposition 4.1 the term $W_{M(k)}\big(\lambda(\boldsymbol{m})\big)$ ensures ellipticity of $\mathbf{b}(\boldsymbol{m}; \cdot, \cdot)$.

(iii) While $\boldsymbol{\pi}(\boldsymbol{v})$ in (4.4a) stems from the formal derivation $\partial_t(\boldsymbol{\pi}(\boldsymbol{m})) = \boldsymbol{\pi}(\boldsymbol{m}_t)$ and (4.1), the term $\boldsymbol{D}(\boldsymbol{m}, \boldsymbol{v})$ stems from the corresponding $\partial_t(\boldsymbol{\Pi}(\boldsymbol{m})) = \boldsymbol{D}(\boldsymbol{m}, \boldsymbol{v})$ and (4.1). Note that (4.4a) corresponds to (2.10) in combination with (2.12) and requires the evaluation of $\boldsymbol{\pi}(\boldsymbol{v})$ and $\boldsymbol{D}(\boldsymbol{m}, \boldsymbol{v})$. However, (4.4b) follows from (4.4a) with $\boldsymbol{v}(t) := \boldsymbol{m}_t(t) + \mathcal{O}(k)$ from (4.1) and avoids these evaluations.

5. Proof of Theorem 2.2 (Numerical integration of LLG)

Proof. of Theorem 2.2(i) Together with the Lax–Milgram theorem, (2.10) is solved by a fixed-point iteration with $\boldsymbol{\eta}_h^\ell \approx \boldsymbol{v}_h^i$: Let $\boldsymbol{\eta}_h^0 := \mathbf{0}$. For $\ell \in \mathbb{N}_0$ let $\boldsymbol{\eta}_h^{\ell+1} \in \mathcal{K}_h(\boldsymbol{m}_h^i)$ solve

$$\begin{aligned}&\langle W_{M(k)}(\lambda_h^i)\, \boldsymbol{\eta}_h^{\ell+1}, \boldsymbol{\varphi}_h \rangle_\omega + \langle \boldsymbol{m}_h^i \times \boldsymbol{\eta}_h^{\ell+1}, \boldsymbol{\varphi}_h \rangle_\omega + \frac{\ell_{\mathrm{ex}}^2}{2} k\,(1+\rho(k)) \langle \nabla \boldsymbol{\eta}_h^{\ell+1}, \nabla \boldsymbol{\varphi}_h \rangle_\omega \\ &\quad = -\ell_{\mathrm{ex}}^2 \langle \nabla \boldsymbol{m}_h^i, \nabla \boldsymbol{\varphi}_h \rangle_\omega + \langle \boldsymbol{f}(t_{i+1/2}), \boldsymbol{\varphi}_h \rangle_\omega + \langle \boldsymbol{\pi}_h^i(\boldsymbol{\eta}_h^\ell; \boldsymbol{m}_h^i, \boldsymbol{m}_h^{i-1}), \boldsymbol{\varphi}_h \rangle_\omega \\ &\qquad + \langle \boldsymbol{\Pi}_h^i(\boldsymbol{\eta}_h^\ell; \boldsymbol{m}_h^i, \boldsymbol{m}_h^{i-1}), \boldsymbol{\varphi}_h \rangle_\omega \quad \text{for all } \boldsymbol{\varphi}_h \in \mathcal{K}_h(\boldsymbol{m}_h^i). \end{aligned} \tag{5.1}$$

We equip $\mathcal{K}_h(\boldsymbol{m}_h^i)$ with the norm $|\!|\!| \boldsymbol{\eta}_h |\!|\!|^2 := (\alpha/4)\, \|\boldsymbol{\eta}_h\|_\omega^2 + (\ell_{\mathrm{ex}}^2/2)\, k\,(1+\rho(k))\, \|\nabla \boldsymbol{\eta}_h\|_\omega^2$. For sufficiently small k, Lemma 4.2(i) and (2.7a) prove that $W_{M(k)}(\cdot) \geq \alpha/2$. Since $\rho(k) \geq 0$ the bilinear form on the left-hand side of (5.1) is positive definite on $\mathcal{K}_h(\boldsymbol{m}_h^i)$, i.e., the fixed-point iteration is well defined. We subtract (5.1) for $\boldsymbol{\eta}_h^{\ell+1}$ from (5.1) for $\boldsymbol{\eta}_h^\ell$ and test with $\boldsymbol{\varphi}_h := \boldsymbol{\eta}_h^{\ell+1} - \boldsymbol{\eta}_h^\ell \in \mathcal{K}_h(\boldsymbol{m}_h^i)$. With (2.15a) and (2.16a) we get

$$\begin{aligned}&\frac{\alpha}{2} \|\boldsymbol{\eta}_h^{\ell+1} - \boldsymbol{\eta}_h^\ell\|_\omega^2 + \frac{\ell_{\mathrm{ex}}^2}{2} k\,(1+\rho(k))\, \|\nabla \boldsymbol{\eta}_h^{\ell+1} - \nabla \boldsymbol{\eta}_h^\ell\|_\omega^2 \\ &\overset{(5.1)}{\leqslant} \|\boldsymbol{\pi}_h^i(\boldsymbol{\eta}_h^\ell; \boldsymbol{m}_h^i, \boldsymbol{m}_h^{i-1}) - \boldsymbol{\pi}_h^i(\boldsymbol{\eta}_h^{\ell-1}; \boldsymbol{m}_h^i, \boldsymbol{m}_h^{i-1})\|_\omega \|\boldsymbol{\eta}_h^{\ell+1} - \boldsymbol{\eta}_h^\ell\|_\omega \\ &\quad + \|\boldsymbol{\Pi}_h^i(\boldsymbol{\eta}_h^\ell; \boldsymbol{m}_h^i, \boldsymbol{m}_h^{i-1}) - \boldsymbol{\Pi}_h^i(\boldsymbol{\eta}_h^{\ell-1}; \boldsymbol{m}_h^i, \boldsymbol{m}_h^{i-1})\|_\omega \|\boldsymbol{\eta}_h^{\ell+1} - \boldsymbol{\eta}_h^\ell\|_\omega \\ &\leqslant \Big[(C_\pi + C_\Pi)\, k\, \|\boldsymbol{\eta}_h^\ell - \boldsymbol{\eta}_h^{\ell-1}\|_\omega + C_\Pi\, k\, \|\nabla(\boldsymbol{\eta}_h^\ell - \boldsymbol{\eta}_h^{\ell-1})\|_\omega \Big] \|\boldsymbol{\eta}_h^{\ell+1} - \boldsymbol{\eta}_h^\ell\|_\omega. \end{aligned}$$

For arbitrary $\delta > 0$, the Young inequality thus yields

$$\begin{aligned}
&\min\left\{1\,,\,2-\frac{1}{\alpha\delta}\,(C_{\boldsymbol{\pi}}+2C_{\boldsymbol{\Pi}})\,k\right\}\,|\!|\!|\boldsymbol{\eta}_h^{\ell+1}-\boldsymbol{\eta}_h^{\ell}|\!|\!|^2\\
&\quad\leqslant\left[\frac{\alpha}{2}-\frac{1}{4\delta}\,(C_{\boldsymbol{\pi}}+2C_{\boldsymbol{\Pi}})\,k\right]\|\boldsymbol{\eta}_h^{\ell+1}-\boldsymbol{\eta}_h^{\ell}\|_\omega^2+\frac{\ell_{\mathrm{ex}}^2}{2}\,k\,(1+\rho(k))\,\|\nabla\boldsymbol{\eta}_h^{\ell+1}-\nabla\boldsymbol{\eta}_h^{\ell}\|_\omega^2\\
&\quad\leqslant\delta\,(C_\pi+C_\Pi)\,k\,\|\boldsymbol{\eta}_h^{\ell}-\boldsymbol{\eta}_h^{\ell-1}\|_\omega^2+\delta\,C_{\boldsymbol{\Pi}}\,k\,\|\nabla(\boldsymbol{\eta}_h^{\ell}-\boldsymbol{\eta}_h^{\ell-1})\|_\omega^2\\
&\quad\leqslant\delta\,\max\left\{\frac{4}{\alpha}\,(C_{\boldsymbol{\pi}}+C_{\boldsymbol{\Pi}})\,k\,,\,2\,\frac{C_{\boldsymbol{\Pi}}}{\ell_{\mathrm{ex}}^2}\right\}\,|\!|\!|\boldsymbol{\eta}_h^{\ell}-\boldsymbol{\eta}_h^{\ell-1}|\!|\!|^2\quad\text{for all }\ell\in\mathbb{N}.
\end{aligned}$$

For sufficiently small δ and k the iteration is thus a contraction with respect to $|\!|\!|\cdot|\!|\!|$. The Banach fixed-point theorem yields the existence and uniqueness of the solution $\boldsymbol{v}_h^i\in\mathscr{K}_h(\boldsymbol{m}_h^i)$ to (2.10). For all $z_h\in\mathscr{N}_h$ it holds that $|\boldsymbol{m}_h^i(z_h)+k\,\boldsymbol{v}_h^i(z_h)|^2=1+k^2\,|\boldsymbol{v}_h^i(z_h)|^2\geq 1$ so that $\boldsymbol{m}_h^{i+1}\in\mathscr{M}_h$ in (2.11) is well defined. Altogether, Algorithm 2.2 is thus well posed. □

LEMMA 5.1 Under the assumptions of Theorem 2.2(ii) the following assertions are satisfied, if $k>0$ is sufficiently small.

(i) For all $i=0,\dots,N-1$,

$$\begin{aligned}
&\frac{\ell_{\mathrm{ex}}^2}{2}\,\mathrm{d}_t\,\|\nabla\boldsymbol{m}_h^{i+1}\|_\omega^2+\langle W_{M(k)}(\lambda_h^i)\boldsymbol{v}_h^i,\boldsymbol{v}_h^i\rangle_\omega+\frac{\ell_{\mathrm{ex}}^2}{2}\,k\,\rho(k)\,\|\nabla\boldsymbol{v}_h^i\|_\omega^2\\
&\qquad\leqslant\langle\boldsymbol{f}(t_{i+1/2}),\boldsymbol{v}_h^i\rangle_\omega+\langle\boldsymbol{\pi}_h^i(\boldsymbol{v}_h^i;\boldsymbol{m}_h^i,\boldsymbol{m}_h^{i-1}),\boldsymbol{v}_h^i\rangle_\omega+\langle\boldsymbol{\Pi}_h^i(\boldsymbol{v}_h^i;\boldsymbol{m}_h^i,\boldsymbol{m}_h^{i-1}),\boldsymbol{v}_h^i\rangle_\omega.
\end{aligned}$$

(ii) For all $j=0,\dots,N$,

$$\|\nabla\boldsymbol{m}_h^j\|_\omega^2+k\sum_{i=0}^{j-1}\|\boldsymbol{v}_h^i\|_\omega^2+k^2\rho(k)\sum_{i=0}^{j-1}\|\nabla\boldsymbol{v}_h^i\|_\omega^2\leq C\,,\tag{5.2}$$

where $C>0$ only depends on T, ω, α, ℓ_{ex}^2, $\boldsymbol{f}$, $\boldsymbol{\pi}$, $\boldsymbol{\Pi}$, $\boldsymbol{m}^0$ and κ.

Proof. Testing (2.10) with $\boldsymbol{\varphi}_h:=\boldsymbol{v}_h^i\in\mathscr{K}_h(\boldsymbol{m}_h^i)$ we see that

$$\begin{aligned}
&\langle W_{M(k)}(\lambda_h^i)\boldsymbol{v}_h^i,\boldsymbol{v}_h^i\rangle_\omega+\frac{\ell_{\mathrm{ex}}^2}{2}\,k\,\|\nabla\boldsymbol{v}_h^i\|_\omega^2+\frac{\ell_{\mathrm{ex}}^2}{2}\,k\rho(k)\,\|\nabla\boldsymbol{v}_h^i\|_\omega^2\\
&\qquad=-\ell_{\mathrm{ex}}^2\langle\nabla\boldsymbol{m}_h^i,\nabla\boldsymbol{v}_h^i\rangle_\omega+\langle\boldsymbol{f}(t_{i+1/2}),\boldsymbol{v}_h^i\rangle_\omega+\langle(\boldsymbol{\pi}_h^i+\boldsymbol{\Pi}_h^i)(\boldsymbol{v}_h^i;\boldsymbol{m}_h^i,\boldsymbol{m}_h^{i-1}),\boldsymbol{v}_h^i\rangle_\omega.
\end{aligned}\tag{5.3}$$

Since $\mathscr{T}_h$ is weakly acute Bartels (2005, Lemma 3.2) provides the estimate

$$\|\nabla\boldsymbol{m}_h^{i+1}\|_\omega^2\leq\|\nabla(\boldsymbol{m}_h^i+k\boldsymbol{v}_h^i)\|_\omega^2=\|\nabla\boldsymbol{m}_h^i\|_\omega^2+2k\,\langle\nabla\boldsymbol{m}_h^i,\nabla\boldsymbol{v}_h^i\rangle_\omega+k^2\|\nabla\boldsymbol{v}_h^i\|_\omega^2.$$

Rearranging this estimate and multiplying it by $\ell_{\mathrm{ex}}^2/(2k)$ we derive that

$$\frac{\ell_{\mathrm{ex}}^2}{2}\,\mathrm{d}_t\,\|\nabla\boldsymbol{m}_h^{i+1}\|_\omega^2-\frac{\ell_{\mathrm{ex}}^2}{2}\,k\,\|\nabla\boldsymbol{v}_h^i\|_\omega^2\leq\ell_{\mathrm{ex}}^2\langle\nabla\boldsymbol{m}_h^i,\nabla\boldsymbol{v}_h^i\rangle_\omega.\tag{5.4}$$

Adding (5.3) and (5.4) we prove (i).

To prove (ii) we sum (5.2) over $i = 0, \dots, j-1$ and multiply by k. For k sufficiently small we have $W_{M(k)}(\cdot) \geq \alpha/2 > 0$ (see Lemma 4.2(i)) and altogether get

$$\begin{aligned} \chi_{\mathrm{j}} &:= \frac{\ell_{\mathrm{ex}}^2}{2} \|\nabla \boldsymbol{m}_h^j\|_\omega^2 + \frac{\alpha}{2} k \sum_{i=0}^{j-1} \|\boldsymbol{v}_h^i\|_\omega^2 + \frac{\ell_{\mathrm{ex}}^2}{2} k^2 \rho(k) \sum_{i=0}^{j-1} \|\nabla \boldsymbol{v}_h^i\|_\omega^2 \\ &\overset{(5.2)}{\leq} \frac{\ell_{\mathrm{ex}}^2}{2} \|\nabla \boldsymbol{m}_h^0\|_\omega^2 + k \sum_{i=0}^{j-1} \langle \boldsymbol{f}(t_{i+1/2}), \boldsymbol{v}_h^i \rangle_\omega + k \sum_{i=0}^{j-1} \langle (\boldsymbol{\pi}_h^i + \boldsymbol{\Pi}_h^i)(\boldsymbol{v}_h^i; \boldsymbol{m}_h^i, \boldsymbol{m}_h^{i-1}), \boldsymbol{v}_h^i \rangle_\omega. \end{aligned} \tag{5.5}$$

Let $\delta > 0$. The Young inequality proves that

$$k^2 \sum_{i=0}^{j-1} \|\nabla \boldsymbol{v}_h^i\|_\omega \|\boldsymbol{v}_h^i\|_\omega \lesssim \delta k^2 \rho(k) \sum_{i=0}^{j-1} \|\nabla \boldsymbol{v}_h^i\|_\omega^2 + \frac{k^2}{\delta \rho(k)} \sum_{i=0}^{j-1} \|\boldsymbol{v}_h^i\|_\omega^2. \tag{5.6}$$

Together with (2.15b) and (2.16b), further applications of the Young inequality prove that

$$\begin{aligned} \chi_j &\overset{(5.5)}{\lesssim} \|\nabla \boldsymbol{m}_h^0\|_\omega^2 + k \sum_{i=0}^{j-1} \|\boldsymbol{f}(t_{i+1/2})\|_\omega \|\boldsymbol{v}_h^i\|_\omega + k \sum_{i=0}^{j-1} \Big(k \|\boldsymbol{v}_h^i\|_\omega + \|\boldsymbol{m}_h^i\|_\omega + \|\boldsymbol{m}_h^{i-1}\|_\omega \Big) \|\boldsymbol{v}_h^i\|_\omega \\ &\quad + k \sum_{i=0}^{j-1} \Big(k \|\boldsymbol{v}_h^i\|_{\boldsymbol{H}^1(\omega)} + \|\boldsymbol{m}_h^i\|_{\boldsymbol{H}^1(\omega)} + \|\boldsymbol{m}_h^{i-1}\|_{\boldsymbol{H}^1(\omega)} \Big) \|\boldsymbol{v}_h^i\|_\omega \\ &\overset{(5.6)}{\lesssim} \|\nabla \boldsymbol{m}_h^0\|_\omega^2 + \frac{k}{\delta} \sum_{i=0}^{j-1} \|\boldsymbol{f}(t_{i+1/2})\|_\omega^2 + \frac{k}{\delta} \sum_{i=0}^{j-1} \|\boldsymbol{m}_h^i\|_\omega^2 + \frac{k}{\delta} \sum_{i=0}^{j-1} \|\nabla \boldsymbol{m}_h^i\|_\omega^2 \\ &\quad + \Big(\delta + k + \frac{k}{\delta \rho(k)} \Big) k \sum_{i=0}^{j-1} \|\boldsymbol{v}_h^i\|_\omega^2 + \delta\, k^2 \rho(k) \sum_{i=0}^{j-1} \|\nabla \boldsymbol{v}_h^i\|_\omega^2. \end{aligned}$$

Since $k/\rho(k) \to 0$ as $k \to 0$, we choose $\delta > 0$ sufficiently small and can absorb the sums $k \sum_{i=0}^{j-1} \|\boldsymbol{v}_h^i\|_\omega^2$ and $k^2 \rho(k) \sum_{i=0}^{j-1} \|\nabla \boldsymbol{v}_h^i\|_\omega^2$ in χ_j. Using that $\boldsymbol{f} \in C^1([0,T], \boldsymbol{L}^2(\omega))$ we altogether arrive at the estimate

$$\chi_{\mathrm{j}} \lesssim \|\nabla \boldsymbol{m}_h^0\|_\omega^2 + k \sum_{i=0}^{j-1} \|\boldsymbol{f}(t_{i+1/2})\|_\omega^2 + k \sum_{i=0}^{j-1} \|\boldsymbol{m}_h^i\|_\omega^2 + k \sum_{i=0}^{j-1} \|\nabla \boldsymbol{m}_h^i\|_\omega^2 \lesssim 1 + k \sum_{i=0}^{j-1} \chi_{\mathrm{i}}.$$

This fits in the setting of the discrete Gronwall lemma (see Quarteroni & Valli, 1994, Lemma 1.4.2), i.e.,

$$\chi_j \lesssim \alpha_0 + \beta \sum_{i=0}^{j-1} \chi_i \quad \text{with } \alpha_0 > 0 \text{ and } \beta \simeq k.$$

We obtain $\chi_j \lesssim \alpha_0 \exp(\sum_{i=0}^{j-1} k) \lesssim \exp(T)$. This concludes the proof. □

LEMMA 5.2 Under the assumptions of Theorem 2.2(ii) consider the postprocessed output (2.5) of Algorithm 2.2. Then there exists $\boldsymbol{m} \in \boldsymbol{H}^1(\omega_T) \cap L^\infty(0,T;\boldsymbol{H}^1(\omega))$, as well as a subsequence of each $\boldsymbol{m}_{hk}^\star \in \{\boldsymbol{m}_{hk}, \boldsymbol{m}_{hk}^=, \boldsymbol{m}_{hk}^-, \boldsymbol{m}_{hk}^+\}$ and of $\boldsymbol{v}_{hk}^-$, such that the following convergence statements hold true simultaneously for the same subsequence as $h,k \to 0$:

(i) $\boldsymbol{m}_{hk} \rightharpoonup \boldsymbol{m}$ in $\boldsymbol{H}^1(\omega_T)$,

(ii) $\boldsymbol{m}_{hk}^\star \overset{*}{\rightharpoonup} \boldsymbol{m}$ in $L^\infty(0,T;\boldsymbol{H}^1(\omega))$,

(iii) $\boldsymbol{m}_{hk}^\star \rightharpoonup \boldsymbol{m}$ in $L^2(0,T;\boldsymbol{H}^1(\omega))$,

(iv) $\boldsymbol{m}_{hk}^\star \to \boldsymbol{m}$ in $\boldsymbol{L}^2(\omega_T)$,

(v) $\boldsymbol{m}_{hk}^\star(t) \to \boldsymbol{m}(t)$ in $\boldsymbol{L}^2(\omega)$ for $t \in (0,T)$ a.e.,

(vi) $\boldsymbol{m}_{hk}^\star \to \boldsymbol{m}$ pointwise a.e. in ω_T,

(vii) $\boldsymbol{v}_{hk}^- \rightharpoonup \partial_t \boldsymbol{m}$ in $\boldsymbol{L}^2(\omega_T)$,

(viii) $k\,\nabla \boldsymbol{v}_{hk}^- \to 0$ in $\boldsymbol{L}^2(\omega_T)$.

Proof. Lemma 5.1 yields uniform boundedness of $\boldsymbol{m}_{hk}$ in $\boldsymbol{H}^1(\omega_T)$ and of $\boldsymbol{m}_{hk}^\star \in L^\infty(0,T;\boldsymbol{H}^1(\omega))$. Therefore, (i)–(vii) follow as in Alouges (2008); Bruckner *et al.* (2014). Lemma 5.1(ii) yields

$$k^2 \|\nabla \boldsymbol{v}_{hk}^-\|_{\boldsymbol{L}^2(\omega_T)}^2 = k\rho(k)^{-1}\rho(k)k^2 \sum_{i=0}^{N-1} \|\nabla \boldsymbol{v}_h^i\|_\omega^2 \overset{(5.2)}{\lesssim} k\rho(k)^{-1} \overset{(2.7b)}{\longrightarrow} 0 \quad \text{as} h,k \to 0. \tag{5.7}$$

This proves (viii) and concludes the proof. □

REMARK 5.1 Under the CFL condition $k = \mathbf{o}(h)$, one may choose $\rho(k) \equiv 0$ and hence violate (2.7b). To see this, note that (2.7b) is only used for the proofs of (5.6) and (5.7). An inverse inequality yields

$$k^2 \sum_{i=0}^{j-1} \|\nabla \boldsymbol{v}_h^i\|_\omega \|\boldsymbol{v}_h^i\|_\omega \lesssim (kh^{-1})\, k \sum_{i=0}^{j-1} \|\boldsymbol{v}_h^i\|_\omega^2,$$

where $k/h \to 0$ as $k \to 0$. Similarly,

$$k^2 \|\nabla \boldsymbol{v}_{hk}^-\|_{\boldsymbol{L}^2(\omega_T)}^2 = k^3 \sum_{i=0}^{N-1} \|\nabla \boldsymbol{v}_h^i\|_\omega^2 \lesssim k^3 h^{-2} \sum_{i=0}^{N-1} \|\boldsymbol{v}_h^i\|_\omega^2 \overset{(5.2)}{\lesssim} k^2 h^{-2} \longrightarrow 0 \quad \text{as } h,k \to 0.$$

Therefore, Lemma 5.1 and Lemma 5.2 (and hence also Theorem 2.2) remains valid.

Proof of Theorem 2.2(ii). We verify that $\boldsymbol{m} \in \boldsymbol{H}^1(\omega_T) \cap L^\infty(0,T;\boldsymbol{H}^1(\omega))$ from Lemma 5.2 satisfies Definition 2.1(i)–(iii). The modulus constraint $|\boldsymbol{m}| = 1$ a.e. in ω_T, as well as $\boldsymbol{m}(0) = \boldsymbol{m}^0$ in the sense of traces, follows as in Alouges (2008); Bruckner *et al.* (2014). Hence, $\boldsymbol{m}$ satisfies Definition 2.1(i)–(ii).

It remains to prove that $\boldsymbol{m}$ from Lemma 5.2 satisfies the variational formulation (2.3) from Definition 2.1(iii): to that end, let $\boldsymbol{\varphi} \in \boldsymbol{C}^\infty(\overline{\omega_T})$. Let $\mathscr{I}_h : \boldsymbol{C}(\overline{\omega}) \to \boldsymbol{V}_h$ be the (vector-valued) nodal interpolation

operator. For $t \in [t_i, t_{i+1})$ and $i = 0, \dots, N-1$ we test (2.10) with $\mathscr{I}_h\big(\boldsymbol{m}_h^i \times \boldsymbol{\varphi}(t)\big) \in \mathscr{K}_h(\boldsymbol{m}_h^i)$ and integrate over time. With the definition of the postprocessed output (2.5) and $\bar{\boldsymbol{f}}_k(t) := \boldsymbol{f}(t_{i+1/2})$ for $t \in [t_i, t_{i+1})$ we obtain

$$
\begin{aligned}
&I_{hk}^1 + I_{hk}^2 + \frac{\ell_{\mathrm{ex}}^2}{2} I_{hk}^3 \\
&:= \int_0^T \langle W_{M(k)}(\lambda_{hk}^-)\boldsymbol{v}_{hk}^-, \mathscr{I}_h(\boldsymbol{m}_{hk}^- \times \boldsymbol{\varphi})\rangle_\omega \,\mathrm{d}t + \int_0^T \langle \boldsymbol{m}_{hk}^- \times \boldsymbol{v}_{hk}^-, \mathscr{I}_h(\boldsymbol{m}_{hk}^- \times \boldsymbol{\varphi})\rangle_\omega \,\mathrm{d}t \\
&\quad + \frac{\ell_{\mathrm{ex}}^2}{2} k\,(1+\rho(k)) \int_0^T \langle \nabla \boldsymbol{v}_{hk}^-, \nabla \mathscr{I}_h(\boldsymbol{m}_{hk}^- \times \boldsymbol{\varphi})\rangle_\omega \,\mathrm{d}t \\
&\overset{(2.10)}{=} -\ell_{\mathrm{ex}}^2 \int_0^T \langle \nabla \boldsymbol{m}_{hk}^-, \nabla \mathscr{I}_h(\boldsymbol{m}_{hk}^- \times \boldsymbol{\varphi})\rangle_\omega \,\mathrm{d}t + \int_0^T \langle \boldsymbol{\pi}_{hk}^-(\boldsymbol{v}_{hk}^-; \boldsymbol{m}_{hk}^-, \boldsymbol{m}_{hk}^{=}), \mathscr{I}_h(\boldsymbol{m}_{hk}^- \times \boldsymbol{\varphi})\rangle_\omega \,\mathrm{d}t \\
&\quad + \int_0^T \langle \bar{\boldsymbol{f}}_k, \mathscr{I}_h(\boldsymbol{m}_{hk}^- \times \boldsymbol{\varphi})\rangle_\omega \,\mathrm{d}t + \int_0^T \langle \boldsymbol{\Pi}_{hk}^-(\boldsymbol{v}_{hk}^-; \boldsymbol{m}_{hk}^-, \boldsymbol{m}_{hk}^{=}), \mathscr{I}_h(\boldsymbol{m}_{hk}^- \times \boldsymbol{\varphi})\rangle_\omega \,\mathrm{d}t \\
&=: -\ell_{\mathrm{ex}}^2 I_{hk}^4 + I_{hk}^5 + I_{hk}^6 + I_{hk}^7.
\end{aligned} \tag{5.8}
$$

In the following we prove convergence of the integrals from (5.9) towards their continuous counterparts in the variational formulation (2.3): to this end recall the approximation properties of the nodal interpolation operator $\mathscr{I}_h$ and note that $\bar{\boldsymbol{f}}_k \to \boldsymbol{f}$ in $C([0,T]; \boldsymbol{L}^2(\Omega))$. With Lemma 5.2 we get, as in Alouges (2008); Bruckner *et al.* (2014), that

$$
\begin{aligned}
I_{hk}^2 &\longrightarrow \int_0^T \langle \boldsymbol{m} \times \partial_t \boldsymbol{m}, \boldsymbol{m} \times \boldsymbol{\varphi}\rangle_\omega \,\mathrm{d}t = \int_0^T \langle \partial_t \boldsymbol{m}, \boldsymbol{\varphi}\rangle_\omega \,\mathrm{d}t, \\
I_{hk}^4 &\longrightarrow -\int_0^T \langle \boldsymbol{m} \times \nabla \boldsymbol{m}, \nabla \boldsymbol{\varphi}\rangle_\omega \,\mathrm{d}t \quad \text{and} \quad I_{hk}^6 \longrightarrow \int_0^T \langle \boldsymbol{f}, \boldsymbol{m} \times \boldsymbol{\varphi}\rangle_\omega \,\mathrm{d}t
\end{aligned}
$$

as $h, k \to 0$. Since $M(k)k \to 0$, Lemma 4.2(i) yields $W_{M(k)}(\lambda_{hk}^-) \to \alpha$ in $L^\infty(\omega_T)$. Together with the assumption $\rho(k) \to 0$ as $k \to 0$ we get, as in Alouges *et al.* (2014), that

$$
I_{hk}^1 \longrightarrow \alpha \int_0^T \langle \partial_t \boldsymbol{m}, \boldsymbol{m} \times \boldsymbol{\varphi}\rangle_\omega \,\mathrm{d}t \quad \text{and} \quad I_{hk}^3 \to 0 \quad \text{as h, k} \to 0.
$$

With assumptions (2.15c) and (2.16c) on $\boldsymbol{\pi}_{hk}^-$ and $\boldsymbol{\Pi}_{hk}^-$, respectively, we conclude that

$$
\begin{aligned}
I_{hk}^5 &= \int_0^T \langle \boldsymbol{\pi}_{hk}^-(\boldsymbol{v}_{hk}^-; \boldsymbol{m}_{hk}^-, \boldsymbol{m}_{hk}^{=}), \mathscr{I}_h(\boldsymbol{m}_{hk}^- \times \boldsymbol{\varphi})\rangle_\omega \,\mathrm{d}t \overset{(2.15c)}{\longrightarrow} \int_0^T \langle \boldsymbol{\pi}(\boldsymbol{m}), \boldsymbol{m} \times \boldsymbol{\varphi}\rangle_\omega \,\mathrm{d}t, \\
I_{hk}^7 &= \int_0^T \langle \boldsymbol{\Pi}_{hk}^-(\boldsymbol{v}_{hk}^-; \boldsymbol{m}_{hk}^-, \boldsymbol{m}_{hk}^{=}), \mathscr{I}_h(\boldsymbol{m}_{hk}^- \times \boldsymbol{\varphi})\rangle_\omega \,\mathrm{d}t \overset{(2.16c)}{\longrightarrow} \int_0^T \langle \boldsymbol{\Pi}(\boldsymbol{m}), \boldsymbol{m} \times \boldsymbol{\varphi}\rangle_\omega \,\mathrm{d}t,
\end{aligned}
$$

as $h, k \to 0$. Altogether, $\boldsymbol{m}$ from Lemma 5.2 satisfies the variational formulation (2.3). □

Proof of Theorem 2.2(iii). It remains to verify that $\boldsymbol{m}$ from Lemma 5.2 satisfies the energy estimate of Definition 2.1: to that end let $\tau \in (0,T)$ be arbitrary and $j \in \{1,\dots,N\}$ such that $\tau \in [t_{j-1}, t_j)$. Besides the shorthand notation $\boldsymbol{f}^j := \boldsymbol{f}(t_j)$, define the time reconstructions $\boldsymbol{f}_k$ and $\overline{\boldsymbol{f}}_k$ according to (2.5). For any $i = 0,\dots,j-1$, Lemma 5.1(i) shows that

$$
\begin{aligned}
&\mathscr{E}_{\mathrm{LLG}}(\boldsymbol{m}_{hk}(t_{i+1})) - \mathscr{E}_{\mathrm{LLG}}(\boldsymbol{m}_{hk}(t_i)) \\
&\quad\overset{(2.2)}{=}\ \frac{\ell_{\mathrm{ex}}^2}{2}\,\|\nabla \boldsymbol{m}_h^{i+1}\|_\omega^2 - \frac{\ell_{\mathrm{ex}}^2}{2}\,\|\nabla \boldsymbol{m}_h^{i}\|_\omega^2 \\
&\qquad -\frac{1}{2}\,\langle \boldsymbol{\pi}(\boldsymbol{m}_h^{i+1}), \boldsymbol{m}_h^{i+1}\rangle_\omega + \frac{1}{2}\,\langle \boldsymbol{\pi}(\boldsymbol{m}_h^{i}), \boldsymbol{m}_h^{i}\rangle_\omega - \langle \boldsymbol{f}^{i+1}, \boldsymbol{m}_h^{i+1}\rangle_\omega + \langle \boldsymbol{f}^{i}, \boldsymbol{m}_h^{i}\rangle_\omega \\
&\quad\overset{(5.2)}{\leqslant}\ -k\,\langle W_{M(k)}(\lambda_h^i)\boldsymbol{v}_h^i, \boldsymbol{v}_h^i\rangle_\omega - \frac{\ell_{\mathrm{ex}}^2}{2}\,k^2\rho(k)\,\|\nabla \boldsymbol{v}_h^i\|_\omega^2 + k\,\langle \boldsymbol{\Pi}_h^i(\boldsymbol{v}_h^i; \boldsymbol{m}_h^i, \boldsymbol{m}_h^{i-1}), \boldsymbol{v}_h^i\rangle_\omega \\
&\qquad \underbrace{+\,k\,\langle \boldsymbol{\pi}_h^i(\boldsymbol{v}_h^i; \boldsymbol{m}_h^i, \boldsymbol{m}_h^{i-1}), \boldsymbol{v}_h^i\rangle_\omega - \frac{1}{2}\,\langle \boldsymbol{\pi}(\boldsymbol{m}_h^{i+1}), \boldsymbol{m}_h^{i+1}\rangle_\omega + \frac{1}{2}\,\langle \boldsymbol{\pi}(\boldsymbol{m}_h^{i}), \boldsymbol{m}_h^{i}\rangle_\omega}_{=:T_{\boldsymbol{\pi}}} \\
&\qquad \underbrace{+\,k\,\langle \boldsymbol{f}(t_{i+1/2}), \boldsymbol{v}_h^i\rangle_\omega - \langle \boldsymbol{f}^{i+1}, \boldsymbol{m}_h^{i+1}\rangle_\omega + \langle \boldsymbol{f}^{i}, \boldsymbol{m}_h^{i}\rangle_\omega}_{=:T_f}\,.
\end{aligned}
\tag{5.9}
$$

Since $\boldsymbol{\pi}$ is linear and self-adjoint we obtain

$$
\begin{aligned}
T_{\boldsymbol{\pi}} &= -\frac{1}{2}\,\langle \boldsymbol{\pi}(\boldsymbol{m}_h^{i+1}), \boldsymbol{m}_h^{i+1}\rangle_\omega + \frac{1}{2}\,\langle \boldsymbol{\pi}(\boldsymbol{m}_h^{i}), \boldsymbol{m}_h^{i}\rangle_\omega + k\,\langle \boldsymbol{\pi}_h^i(\boldsymbol{v}_h^i; \boldsymbol{m}_h^i, \boldsymbol{m}_h^{i-1}), \boldsymbol{v}_h^i\rangle_\omega \\
&= k\,\langle \boldsymbol{\pi}_h^i(\boldsymbol{v}_h^i; \boldsymbol{m}_h^i, \boldsymbol{m}_h^{i-1}) - \boldsymbol{\pi}(\boldsymbol{m}_h^i), \boldsymbol{v}_h^i\rangle_\omega - \langle \boldsymbol{\pi}(\boldsymbol{m}_h^i), \boldsymbol{m}_h^{i+1} - \boldsymbol{m}_h^i - k\boldsymbol{v}_h^i\rangle \\
&\quad -\frac{1}{2}\,\langle \boldsymbol{\pi}(\boldsymbol{m}_h^{i+1} - \boldsymbol{m}_h^i), \boldsymbol{m}_h^{i+1} - \boldsymbol{m}_h^i\rangle_\omega.
\end{aligned}
\tag{5.10}
$$

Similarly,

$$
\begin{aligned}
T_{\boldsymbol{f}} &= k\,\langle \boldsymbol{f}(t_{i+1/2}), \boldsymbol{v}_h^i\rangle_\omega - k\,\langle \mathrm{d}_t \boldsymbol{f}^{i+1}, \boldsymbol{m}_h^i\rangle_\omega - \langle \boldsymbol{f}^{i+1}, \boldsymbol{m}_h^{i+1} - \boldsymbol{m}_h^i\rangle_\omega \\
&= k\,\langle \boldsymbol{f}(t_{i+1/2}) - \boldsymbol{f}^{i+1}, \boldsymbol{v}_h^i\rangle_\omega - k\,\langle \mathrm{d}_t \boldsymbol{f}^{i+1}, \boldsymbol{m}_h^i\rangle_\omega - \langle \boldsymbol{f}^{i+1}, \boldsymbol{m}_h^{i+1} - \boldsymbol{m}_h^i - k\boldsymbol{v}_h^i\rangle_\omega \\
&=: T_{\boldsymbol{f},1} - k\,\langle \mathrm{d}_t \boldsymbol{f}^{i+1}, \boldsymbol{m}_h^i\rangle_\omega + T_{\boldsymbol{f},2}.
\end{aligned}
$$

Elementary calculations show that

$$
|\boldsymbol{m}_h^{i+1}(z_h) - \boldsymbol{m}_h^i(z_h)| \leq k\,|\boldsymbol{v}_h^i(z_h)| \quad \text{for all } z_h \in \mathscr{N}_h.
$$

A scaling argument thus proves that

$$
k\,\|\mathrm{d}_t \boldsymbol{m}_h^{i+1}\|_{\boldsymbol{L}^2(\omega)} = \|\boldsymbol{m}_h^{i+1} - \boldsymbol{m}_h^i\|_{\boldsymbol{L}^2(\omega)} \lesssim k\,\|\boldsymbol{v}_h^i\|_{\boldsymbol{L}^2(\omega)}.
\tag{5.11}
$$

Elementary calculations (see, e.g., Alouges & Jaisson, 2006, eq. (22)) show that

$$|\boldsymbol{m}_h^{i+1}(z_h) - \boldsymbol{m}_h^i(z_h) - k\,\boldsymbol{v}_h^i(z_h)| \le \frac{k^2}{2}\,|\boldsymbol{v}_h^i(z_h)|^2 \quad \text{for all } z_h \in \mathcal{N}_h.$$

A scaling argument thus proves that

$$k\,\|\mathrm{d}_t\,\boldsymbol{m}_h^{i+1} - \boldsymbol{v}_h^i\|_{\boldsymbol{L}^p(\omega)} = \|\boldsymbol{m}_h^{i+1} - \boldsymbol{m}_h^i - k\,\boldsymbol{v}_h^i\|_{\boldsymbol{L}^p(\omega)} \lesssim k^2\,\|\boldsymbol{v}_h^i\|^2_{\boldsymbol{L}^{2p}(\omega)} \text{for } 1 \le p < \infty. \tag{5.12}$$

The Sobolev embedding $\boldsymbol{H}^1(\omega) \subset \boldsymbol{L}^6(\omega)$ yields

$$\|\boldsymbol{v}_h^i\|^2_{\boldsymbol{L}^3(\omega)} \le \|\boldsymbol{v}_h^i\|_{\boldsymbol{L}^2(\omega)}\,\|\boldsymbol{v}_h^i\|_{\boldsymbol{L}^6(\omega)} \lesssim \|\boldsymbol{v}_h^i\|_{\boldsymbol{L}^2(\omega)}\,\|\boldsymbol{v}_h^i\|_{\boldsymbol{H}^1(\omega)} \le \|\boldsymbol{v}_h^i\|_\omega^2 + \|\boldsymbol{v}_h^i\|_\omega\,\|\nabla \boldsymbol{v}_h^i\|_\omega.$$

Therefore, we obtain

$$\|\boldsymbol{m}_h^{i+1} - \boldsymbol{m}_h^i - k\boldsymbol{v}_h^i\|_{\boldsymbol{L}^{3/2}(\omega)} \overset{(5.12)}{\lesssim} k^2\,\|\boldsymbol{v}_h^i\|^2_{\boldsymbol{L}^3(\omega)} \lesssim k^2\,\|\boldsymbol{v}_h^i\|_\omega \|\nabla \boldsymbol{v}_h^i\|_\omega + k^2\,\|\boldsymbol{v}_h^i\|_\omega^2.$$

With the stronger boundedness (2.17) of $\boldsymbol{\pi}$ and the Hölder inequality we derive that

$$\begin{aligned}
|T_{\boldsymbol{\pi}}| &\overset{(5.10)}{\lesssim} k\,|\langle \boldsymbol{\pi}_h^i(\boldsymbol{v}_h^i; \boldsymbol{m}_h^i, \boldsymbol{m}_h^{i-1}) - \boldsymbol{\pi}(\boldsymbol{m}_h^i), \boldsymbol{v}_h^i\rangle_\omega| \\
&\quad + \|\boldsymbol{\pi}(\boldsymbol{m}_h^i)\|_{\boldsymbol{L}^3(\omega)}\,\|\boldsymbol{m}_h^{i+1} - \boldsymbol{m}_h^i - k\boldsymbol{v}_h^i\|_{\boldsymbol{L}^{3/2}(\omega)} + \|\boldsymbol{\pi}(\boldsymbol{m}_h^{i+1} - \boldsymbol{m}_h^i)\|_\omega\,\|\boldsymbol{m}_h^{i+1} - \boldsymbol{m}_h^i\|_\omega \\
&\lesssim k\,|\langle \boldsymbol{\pi}_h^i(\boldsymbol{v}_h^i; \boldsymbol{m}_h^i, \boldsymbol{m}_h^{i-1}) - \boldsymbol{\pi}(\boldsymbol{m}_h^i), \boldsymbol{v}_h^i\rangle_\omega| + k^2\,\|\boldsymbol{v}_h^i\|_\omega \|\nabla \boldsymbol{v}_h^i\|_\omega + k^2\,\|\boldsymbol{v}_h^i\|_\omega^2.
\end{aligned} \tag{5.13}$$

Similarly, the additional assumption $\boldsymbol{f} \in C^1([0,T]; \boldsymbol{L}^2(\omega)) \cap C([0,T]; \boldsymbol{L}^3(\omega))$ yields

$$|T_{\boldsymbol{f},1} + T_{\boldsymbol{f},2}| \lesssim k|\langle \boldsymbol{f}(t_{i+1/2}) - \boldsymbol{f}^{i+1}, \boldsymbol{v}_h^i\rangle_\omega| + k^2\,\|\boldsymbol{v}_h^i\|_\omega \|\nabla \boldsymbol{v}_h^i\|_\omega + k^2\,\|\boldsymbol{v}_h^i\|_\omega^2. \tag{5.14}$$

The combination of (5.9) with (5.13)–(5.14) and summation over $i = 0, \dots, j-1$ yields

$$\begin{aligned}
&\mathscr{E}_{\mathrm{LLG}}(\boldsymbol{m}_{hk}^+(\tau)) - \mathscr{E}_{\mathrm{LLG}}(\boldsymbol{m}_h^0) + \int_0^{t_j} \langle W_{M(k)}(\lambda_{hk}^-)\boldsymbol{v}_{hk}^-, \boldsymbol{v}_{hk}^-\rangle_\omega\,\mathrm{d}t \\
&\quad + \int_0^{t_j} \langle \partial_t \boldsymbol{f}_k, \boldsymbol{m}_{hk}^-\rangle_\omega\,\mathrm{d}t - \int_0^{t_j} \langle \boldsymbol{\Pi}_{hk}(\boldsymbol{v}_{hk}^-; \boldsymbol{m}_{hk}^-, \boldsymbol{m}_{hk}^=), \boldsymbol{v}_{hk}^-\rangle_\omega\,\mathrm{d}t \\
&\lesssim k\int_0^{t_j} \|\boldsymbol{v}_{hk}^-\|_\omega^2\,\mathrm{d}t + k\int_0^{t_j} \|\boldsymbol{v}_{hk}^-\|_\omega \|\nabla \boldsymbol{v}_{hk}^-\|_\omega\,\mathrm{d}t \\
&\quad + \int_0^{t_j} |\langle \boldsymbol{\pi}_{hk}(\boldsymbol{v}_{hk}^-; \boldsymbol{m}_{hk}^-, \boldsymbol{m}_{hk}^=) - \boldsymbol{\pi}(\boldsymbol{m}_{hk}^-), \boldsymbol{v}_h^j\rangle_\omega|\,\mathrm{d}t + \int_0^{t_j} |\langle \bar{\boldsymbol{f}}_k - \boldsymbol{f}_k^+, \boldsymbol{v}_{hk}^-\rangle_\omega|\,\mathrm{d}t\,.
\end{aligned} \tag{5.15}$$

From strong convergence in (2.14) it follows that $\mathscr{E}_{\mathrm{LLG}}(\boldsymbol{m}_h^0) \to \mathscr{E}_{\mathrm{LLG}}(\boldsymbol{m}^0)$ as $h, k \to 0$. The first and second terms on the right-hand side vanish as $h, k \to 0$ due to Lemma 5.2(vii)–(viii). Thanks to

(2.15c) and (2.16c) with strong convergence, the last two terms on the right-hand side of (5.15) vanish as $h, k \to 0$. Standard lower semicontinuity arguments for the remaining terms in (5.15) conclude the proof. □

6. Proof of Theorem 3.2 (Numerical integration of ELLG)

Proof of Theorem 3.2(i). Note that the right-hand side of (3.5a) can depend nonlinearly on $\boldsymbol{v}_h^i$. As in the proof of Theorem 2.2(i) we employ a fixed-point iteration, where $(\boldsymbol{\eta}_h^\ell, \boldsymbol{v}_h^\ell) \approx (\boldsymbol{v}_h^i, \boldsymbol{h}_h^{i+1/2}) \in \mathscr{K}_h(\boldsymbol{m}_h^i) \times \mathscr{X}_h$. To this end let $\boldsymbol{\eta}_h^0 := 0$ and $\boldsymbol{v}_h^0 := \boldsymbol{h}_h^i$. For $\ell \in \mathbb{N}_0$ let $\boldsymbol{\eta}_h^{\ell+1} \in \mathscr{K}_h(\boldsymbol{m}_h^i)$ satisfy, for all $\boldsymbol{\varphi}_h \in \mathscr{K}_h(\boldsymbol{m}_h^i)$,

$$\begin{aligned}
&\langle W_{M(k)}(\lambda_h^i)\boldsymbol{\eta}_h^{\ell+1}, \boldsymbol{\varphi}_h\rangle_\omega + \langle \boldsymbol{m}_h^i \times \boldsymbol{\eta}_h^{\ell+1}, \boldsymbol{\varphi}_h\rangle_\omega + \frac{\ell_{\mathrm{ex}}^2}{2}\, k\,(1+\rho(k))\langle \nabla\boldsymbol{\eta}_h^{\ell+1}, \nabla\boldsymbol{\varphi}_h\rangle_\omega \\
&= -\ell_{\mathrm{ex}}^2\langle \nabla\boldsymbol{m}_h^i, \nabla\boldsymbol{\varphi}_h\rangle_\omega + \langle \boldsymbol{\pi}_h^i(\boldsymbol{\eta}_h^\ell; \boldsymbol{m}_h^i, \boldsymbol{m}_h^{i-1}), \boldsymbol{\varphi}_h\rangle_\omega + \langle \boldsymbol{f}_h^{i+1/2}, \boldsymbol{\varphi}_h\rangle_\omega \\
&\quad + \langle \boldsymbol{\Pi}_h^i(\boldsymbol{\eta}_h^\ell; \boldsymbol{m}_h^i, \boldsymbol{m}_h^{i-1}), \boldsymbol{\varphi}_h\rangle_\omega + 2\boldsymbol{\Theta}_{i3}^k\langle \boldsymbol{v}_h^\ell, \boldsymbol{\varphi}_h\rangle_\omega + \langle (\boldsymbol{\Theta}_{i2}^k - \boldsymbol{\Theta}_{i3}^k)\boldsymbol{h}_h^i + \boldsymbol{\Theta}_{i1}^k \boldsymbol{h}_h^{i-1}, \boldsymbol{\varphi}_h\rangle_\omega.
\end{aligned} \tag{6.1a}$$

With $\mathscr{I}_h$ being the nodal interpolation operator let $\boldsymbol{v}_h^{\ell+1} \in \mathscr{X}_h$ satisfy, for all $\boldsymbol{\zeta}_h \in \mathscr{X}_h$,

$$\begin{aligned}
&\frac{2\mu_0}{k}\langle \boldsymbol{v}_h^{\ell+1}, \boldsymbol{\zeta}_h\rangle_\Omega + \langle \sigma^{-1}\nabla \times \boldsymbol{v}_h^{\ell+1}, \nabla \times \boldsymbol{\zeta}_h\rangle_\Omega \\
&\quad = -\frac{\mu_0}{k}\left\langle \mathscr{I}_h\left(\frac{\boldsymbol{m}_h^i + k\boldsymbol{\eta}_h^{\ell+1}}{|\boldsymbol{m}_h^i + k\boldsymbol{\eta}_h^{\ell+1}|}\right), \boldsymbol{\zeta}_h\right\rangle_\omega + \frac{\mu_0}{k}\langle \boldsymbol{m}_h^i, \boldsymbol{\zeta}_h\rangle_\omega + \frac{2\mu_0}{k}\langle \boldsymbol{h}_h^i, \boldsymbol{\zeta}_h\rangle_\Omega.
\end{aligned} \tag{6.1b}$$

Since $\rho(k) \geq 0$ and $W_{M(k)}(\cdot) > 0$, the bilinear forms on the left-hand sides of (6.1) are elliptic on $(\mathscr{K}_h(\boldsymbol{m}_h^i), \|\cdot\|_\omega)$ and $(\mathscr{X}_h, \|\cdot\|_\Omega)$, respectively. Since $\boldsymbol{\eta}_h^{\ell+1}$ is known for the computation of $\boldsymbol{v}_h^{\ell+1}$ the fixed-point iteration is thus well defined. We subtract (6.1) for $(\boldsymbol{\eta}_h^\ell, \boldsymbol{v}_h^\ell)$ from (6.1) for $(\boldsymbol{\eta}_h^{\ell+1}, \boldsymbol{v}_h^{\ell+1})$ and test with $\boldsymbol{\varphi}_h := \boldsymbol{\eta}_h^{\ell+1} - \boldsymbol{\eta}_h^\ell \in \mathscr{K}_h(\boldsymbol{m}_h^i)$ and $\boldsymbol{\zeta}_h := \boldsymbol{v}_h^{\ell+1} - \boldsymbol{v}_h^\ell \in \mathscr{X}_h$. For sufficiently small k, Lemma 4.2(i) and (2.7a) prove that $W_{M(k)}(\cdot) \geq \alpha/2$. With $\sup_k \max_{ij} |\boldsymbol{\Theta}_{ij}^k| \leq C_{\boldsymbol{\Theta}} < \infty$ as well as (2.15a) and (2.16a), we get, as in the proof of Theorem 2.2(i), that

$$\begin{aligned}
&\frac{\alpha}{2}\,\|\boldsymbol{\eta}_h^{\ell+1} - \boldsymbol{\eta}_h^\ell\|_\omega^2 + \frac{\ell_{\mathrm{ex}}^2}{2}\,k\,(1+\rho(k))\,\|\nabla(\boldsymbol{\eta}_h^{\ell+1} - \boldsymbol{\eta}_h^\ell)\|_\omega^2 \\
&\overset{(6.1a)}{\leq} \big(C_{\boldsymbol{\pi}} + C_{\boldsymbol{\Pi}}\big)\,k\,\|\boldsymbol{\eta}_h^\ell - \boldsymbol{\eta}_h^{\ell-1}\|_\omega \|\boldsymbol{\eta}_h^{\ell+1} - \boldsymbol{\eta}_h^\ell\|_\omega + C_{\boldsymbol{\Pi}}\,k\,\|\nabla(\boldsymbol{\eta}_h^\ell - \boldsymbol{\eta}_h^{\ell-1})\|_\omega \|\boldsymbol{\eta}_h^{\ell+1} - \boldsymbol{\eta}_h^\ell\|_\omega \\
&\quad + 2C_{\boldsymbol{\Theta}}\|\boldsymbol{v}_h^\ell - \boldsymbol{v}_h^{\ell-1}\|_\Omega \|\boldsymbol{\eta}_h^{\ell+1} - \boldsymbol{\eta}_h^\ell\|_\omega \quad \text{for all } \ell \in \mathbb{N}.
\end{aligned} \tag{6.2}$$

For all $\boldsymbol{\varphi}_h \in \boldsymbol{V}_h$ it holds that $\|\mathscr{I}_h\boldsymbol{\varphi}_h\|_\omega \leq \sqrt{5}\,\|\boldsymbol{\varphi}_h\|_\omega$. Moreover, for all $x, y \in \mathbb{R}$ with $|x|, |y| \geq 1$, it holds that $|x/|x| - y/|y|| \leq |x - y|$. Since $|\boldsymbol{m}_h^i(z_h) + k\boldsymbol{\eta}_h^\ell(z_h)| \geq 1$ for all $\ell \in \mathbb{N}_0$ and for all nodes $z_h \in \mathscr{N}_h|_\omega$,

we get

$$\begin{aligned}
&\|\boldsymbol{v}_h^{\ell+1} - \boldsymbol{v}_h^{\ell}\|_\Omega^2 + \frac{k}{2\mu_0}\|\sigma^{-1/2}\nabla\times\big(\boldsymbol{v}_h^{\ell+1} - \boldsymbol{v}_h^{\ell}\big)\|_\Omega^2 \\
&\quad\overset{(6.1b)}{=} -\frac{1}{2}\left\langle \mathscr{I}_h\left(\frac{\boldsymbol{m}_h^i + k\boldsymbol{\eta}_h^{\ell+1}}{|\boldsymbol{m}_h^i + k\boldsymbol{\eta}_h^{\ell+1}|}\right) - \mathscr{I}_h\left(\frac{\boldsymbol{m}_h^i + k\boldsymbol{\eta}_h^{\ell}}{|\boldsymbol{m}_h^i + k\boldsymbol{\eta}_h^{\ell}|}\right), \boldsymbol{v}_h^{\ell+1} - \boldsymbol{v}_h^{\ell}\right\rangle_\omega \\
&\quad\le \frac{\sqrt{5}k}{2}\,k\,\|\boldsymbol{\eta}_h^{\ell+1} - \boldsymbol{\eta}_h^{\ell}\|_\omega\|\boldsymbol{v}_h^{\ell+1} - \boldsymbol{v}_h^{\ell}\|_\Omega \quad \text{for all } \ell\in\mathbb{N}_0.
\end{aligned}$$

The latter equation yields

$$\|\boldsymbol{v}_h^{\ell+1} - \boldsymbol{v}_h^{\ell}\|_\Omega \leqslant \frac{\sqrt{5}}{2}\,k\,\|\boldsymbol{\eta}_h^{\ell+1} - \boldsymbol{\eta}_h^{\ell}\|_\omega \quad \text{for all } \ell\in\mathbb{N}_0. \tag{6.3}$$

We add (6.2)–(6.3) and obtain

$$\begin{aligned}
&\frac{\alpha}{2}\,\|\boldsymbol{\eta}_h^{\ell+1} - \boldsymbol{\eta}_h^{\ell}\|_\omega^2 + \frac{\ell_{\mathrm{ex}}^2}{2}\,k\,(1+\rho(k))\,\|\nabla(\boldsymbol{\eta}_h^{\ell+1} - \boldsymbol{\eta}_h^{\ell})\|_\omega^2 + \|\boldsymbol{v}_h^{\ell+1} - \boldsymbol{v}_h^{\ell}\|_\Omega^2 \\
&\quad\le \big(C_{\boldsymbol{\pi}} + C_{\boldsymbol{\Pi}} + \sqrt{5}\,C_{\boldsymbol{\Theta}}\big)\,k\,\|\boldsymbol{\eta}_h^{\ell} - \boldsymbol{\eta}_h^{\ell-1}\|_\omega\|\boldsymbol{\eta}_h^{\ell+1} - \boldsymbol{\eta}_h^{\ell}\|_\omega \\
&\qquad + C_{\boldsymbol{\Pi}}\,k\,\|\nabla(\boldsymbol{\eta}_h^{\ell} - \boldsymbol{\eta}_h^{\ell-1})\|_\omega\|\boldsymbol{\eta}_h^{\ell+1} - \boldsymbol{\eta}_h^{\ell}\|_\omega + \frac{5}{4}\,k^2\,\|\boldsymbol{\eta}_h^{\ell+1} - \boldsymbol{\eta}_h^{\ell}\|_\omega^2 \quad \text{for all } \ell\in\mathbb{N}.
\end{aligned}$$

We equip the product space $\mathscr{K}_h(\boldsymbol{m}_h^i)\times\mathscr{X}_h$ with the norm $|\!|\!|(\boldsymbol{\eta}_h,\boldsymbol{v}_h)|\!|\!|^2 := (\alpha/4)\,\|\boldsymbol{\eta}_h\|_\omega^2 + (\ell_{\mathrm{ex}}^2/2)\,k\,(1+\rho(k))\,\|\nabla\boldsymbol{\eta}_h\|_\omega^2 + \|\boldsymbol{v}_h\|_\Omega^2$. For $\delta>0$ the Young inequality then proves that

$$\begin{aligned}
&\min\left\{1\,,\,2 - \frac{1}{\alpha\delta}\,(C_{\boldsymbol{\pi}} + 2C_{\boldsymbol{\Pi}} + \sqrt{5}\,C_{\boldsymbol{\Theta}})\,k - \frac{5}{\alpha}\,k^2\right\}|\!|\!|(\boldsymbol{\eta}_h^{\ell+1},\boldsymbol{v}_h^{\ell+1}) - (\boldsymbol{\eta}_h^{\ell},\boldsymbol{v}_h^{\ell})|\!|\!|^2 \\
&\quad\le \left[\frac{\alpha}{2} - \frac{1}{4\delta}\,(C_{\boldsymbol{\pi}} + 2C_{\boldsymbol{\Pi}} + \sqrt{5}\,C_{\boldsymbol{\Theta}})\,k - \frac{5}{4}\,k^2\right]\|\boldsymbol{\eta}_h^{\ell+1} - \boldsymbol{\eta}_h^{\ell}\|_\omega^2 \\
&\qquad + \frac{\ell_{\mathrm{ex}}^2}{2}\,k\,(1+\rho(k))\,\|\nabla\boldsymbol{\eta}_h^{\ell+1} - \nabla\boldsymbol{\eta}_h^{\ell}\|_\omega^2 + \|\boldsymbol{v}_h^{\ell+1} - \boldsymbol{v}_h^{\ell}\|_\Omega^2 \\
&\quad\le \delta\,\max\left\{\frac{4}{\alpha}\,(C_{\boldsymbol{\pi}} + C_{\boldsymbol{\Pi}} + \sqrt{5}\,C_{\boldsymbol{\Theta}})\,k\,,\,2\,\frac{C_{\boldsymbol{\Pi}}}{\ell_{\mathrm{ex}}^2}\right\}|\!|\!|(\boldsymbol{\eta}_h^{\ell},\boldsymbol{v}_h^{\ell}) - (\boldsymbol{\eta}_h^{\ell-1},\boldsymbol{v}_h^{\ell-1})|\!|\!|^2 \quad \text{for all } \ell\in\mathbb{N}.
\end{aligned}$$

For sufficiently small δ and k the iteration is thus a contraction with respect to $|\!|\!|\cdot|\!|\!|$. The Banach fixed-point theorem yields existence and uniqueness of a fixed point $(\boldsymbol{v}_h^i, \boldsymbol{h}_h^{i+1/2}) \in \mathscr{K}_h(\boldsymbol{m}_h^i)\times\mathscr{X}_h$ of (6.1). With $\boldsymbol{h}_h^{i+1} := 2\boldsymbol{h}_h^{i+1/2} - \boldsymbol{h}_h^i \in \mathscr{X}_h$, $(\boldsymbol{v}_h^i, \boldsymbol{h}_h^{i+1}) \in \mathscr{K}_h(\boldsymbol{m}_h^i)\times\mathscr{X}_h$ is the unique solution of (3.5); see Remark 3.1(vi). The remainder of the proof follows as for Theorem 2.2(i). □

LEMMA 6.1 Under the assumptions of Theorem 3.2(ii) the following assertions are satisfied, if $k>0$ is sufficiently small.

(i) For all $i = 0, \dots, N-1$,

$$\begin{aligned}
&\frac{\ell_{\mathrm{ex}}^2}{2}\,\mathrm{d}_t\,\|\nabla \boldsymbol{m}_h^{i+1}\|_\omega^2 + \langle W_{M(k)}(\lambda_h^i)\boldsymbol{v}_h^i, \boldsymbol{v}_h^i\rangle_\omega + \frac{\ell_{\mathrm{ex}}^2}{2}\,k\rho(k)\,\|\nabla \boldsymbol{v}_h^i\|_\omega^2 \\
&\quad + \frac{1}{2}\,\mathrm{d}_t\,\|\boldsymbol{h}_h^{i+1}\|_\Omega^2 + \frac{1}{\mu_0}\|\sigma^{-1/2}\nabla \times \boldsymbol{h}_h^{i+1/2}\|_\Omega^2 \\
&\le \langle \boldsymbol{f}(t_{i+1/2}), \boldsymbol{v}_h^i\rangle_\omega + \langle \boldsymbol{\pi}_h^i(\boldsymbol{v}_h^i; \boldsymbol{m}_h^i, \boldsymbol{m}_h^{i-1}), \boldsymbol{v}_h^i\rangle_\omega + \langle \boldsymbol{\Pi}_h^i(\boldsymbol{v}_h^i; \boldsymbol{m}_h^i, \boldsymbol{m}_h^{i-1}), \boldsymbol{v}_h^i\rangle_\omega \\
&\quad + \langle \boldsymbol{v}_h^i - \mathrm{d}_t\,\boldsymbol{m}_h^{i+1}, \boldsymbol{h}_h^{i+1/2}\rangle_\omega + \langle \boldsymbol{v}_h^i, \boldsymbol{h}_h^{i,\boldsymbol{\Theta}} - \boldsymbol{h}_h^{i+1/2}\rangle_\omega.
\end{aligned} \tag{6.4}$$

(ii) For all $i = 0, \dots, N-1$,

$$\mu_0 \|\mathrm{d}_t\,\boldsymbol{h}_h^{i+1}\|_\Omega^2 + \mathrm{d}_t\,\|\sigma^{-1/2}\nabla \times \boldsymbol{h}_h^{i+1}\|_\Omega^2 \le \mu_0 \|\mathrm{d}_t\,\boldsymbol{m}_h^{i+1}\|_\omega^2. \tag{6.5}$$

(iii) For all $j = 0, \dots, N-1$,

$$\begin{aligned}
&\|\nabla \boldsymbol{m}_h^j\|_\omega^2 + k\sum_{i=0}^{j-1}\|\boldsymbol{v}_h^i\|_\omega^2 + k^2\rho(k)\sum_{i=0}^{j-1}\|\nabla \boldsymbol{v}_h^i\|_\omega^2 \\
&\qquad + \|\boldsymbol{h}_h^j\|_\Omega^2 + \|\sigma^{-1/2}\nabla \times \boldsymbol{h}_h^j\|_\Omega^2 + k\sum_{i=0}^{j-1}\|\mathrm{d}_t\,\boldsymbol{h}_h^{i+1}\|_\Omega^2 \le C,
\end{aligned} \tag{6.6}$$

where $C > 0$ depends only on T, ω, Ω, α, μ_0, σ_0, ℓ_{ex}^2, $\boldsymbol{f}$, $\boldsymbol{\pi}$, $\boldsymbol{\Pi}$, $\boldsymbol{m}^0$, $\boldsymbol{h}^0$, $C_{\boldsymbol{\Theta}}$ and κ.

Proof. For the LLG part (3.5a), we argue as in the proof of Lemma 5.1(i) to see that

$$\begin{aligned}
&\frac{\ell_{\mathrm{ex}}^2}{2}\,\mathrm{d}_t\,\|\nabla \boldsymbol{m}_h^{i+1}\|_\omega^2 + \langle W_{M(k)}(\lambda_h^i)\boldsymbol{v}_h^i, \boldsymbol{v}_h^i\rangle_\omega + \frac{\ell_{\mathrm{ex}}^2}{2}\,k\rho(k)\,\|\nabla \boldsymbol{v}_h^i\|_\omega^2 \\
&\quad \leqslant \langle \boldsymbol{f}(t_{i+1/2}), \boldsymbol{v}_h^i\rangle_\omega + \langle (\boldsymbol{\pi}_h^i + \boldsymbol{\Pi}_h^i)(\boldsymbol{v}_h^i; \boldsymbol{m}_h^i, \boldsymbol{m}_h^{i-1}), \boldsymbol{v}_h^i\rangle_\omega + \langle \boldsymbol{h}_h^{i,\boldsymbol{\Theta}}, \boldsymbol{v}_h^i\rangle_\Omega.
\end{aligned} \tag{6.7}$$

Testing (3.5b) with $\boldsymbol{\zeta}_h := -(1/\mu_0)\,\boldsymbol{h}_h^{i+1/2}$ we obtain

$$\langle \mathrm{d}_t\,\boldsymbol{m}_h^{i+1}, \boldsymbol{h}_h^{i+1/2}\rangle_\omega \overset{(3.5b)}{=} -\frac{1}{2}\,\mathrm{d}_t\,\|\boldsymbol{h}_h^{i+1}\|_\Omega^2 - \frac{1}{\mu_0}\|\sigma^{-1/2}\nabla \times \boldsymbol{h}_h^{i+1/2}\|_\Omega^2. \tag{6.8}$$

Inserting $\boldsymbol{h}_h^{i,\boldsymbol{\Theta}}$ and $\boldsymbol{v}_h^i$ in (6.8) we are led to

$$\begin{aligned}
\langle \boldsymbol{v}_h^i, \boldsymbol{h}_h^{i,\boldsymbol{\Theta}}\rangle_\omega &= \langle \boldsymbol{v}_h^i, \boldsymbol{h}_h^{i,\boldsymbol{\Theta}} - \boldsymbol{h}_h^{i+1/2}\rangle_\omega + \langle \boldsymbol{v}_h^i - \mathrm{d}_t\,\boldsymbol{m}_h^{i+1}, \boldsymbol{h}_h^{i+1/2}\rangle_\omega \\
&\quad - \frac{1}{2}\,\mathrm{d}_t\,\|\boldsymbol{h}_h^{i+1}\|_\Omega^2 - \frac{1}{\mu_0}\|\sigma^{-1/2}\nabla \times \boldsymbol{h}_h^{i+1/2}\|_\Omega^2.
\end{aligned} \tag{6.9}$$

Adding (6.7) and (6.9) we prove (i). To prove (ii) we test (3.5b) with $\boldsymbol{\zeta}_h := \mathrm{d}_t \boldsymbol{h}_h^{i+1}$. With the Young inequality we obtain

$$\mu_0 \|\mathrm{d}_t \boldsymbol{h}_h^{i+1}\|_\Omega^2 + \frac{1}{2}\,\mathrm{d}_t \|\sigma^{-1/2}\nabla \times \boldsymbol{h}_h^{i+1}\|_\Omega^2 \overset{(3.5b)}{\leqslant} \frac{\mu_0}{2}\|\mathrm{d}_t \boldsymbol{m}_h^{i+1}\|_\omega^2 + \frac{\mu_0}{2}\|\mathrm{d}_t \boldsymbol{h}_h^{i+1}\|_\Omega^2.$$

This proves (ii). To prove (iii) we sum (6.4) over $i = 0, \dots, j-1$ and multiply by k. With $W_{M(k)}(\cdot) \geq \alpha/2 > 0$ for k sufficiently small we obtain

$$\begin{aligned}
\chi_j &:= \frac{\ell_{\mathrm{ex}}^2}{2}\,\|\nabla \boldsymbol{m}_h^j\|_\omega^2 + \frac{\alpha}{2}\,k\sum_{i=0}^{j-1}\|\boldsymbol{v}_h^i\|_\omega^2 + \frac{\ell_{\mathrm{ex}}^2}{2}\,k^2\rho(k)\sum_{i=0}^{j-1}\|\nabla \boldsymbol{v}_h^i\|_\omega^2 \\
&\quad + \frac{1}{2}\,\|\boldsymbol{h}_h^j\|_\Omega^2 + \frac{k}{\mu_0}\sum_{i=0}^{j-1}\|\sigma^{-1/2}\nabla \times \boldsymbol{h}_h^{i+1/2}\|_\Omega^2 \\
&\overset{(6.4)}{\leq} \frac{\ell_{\mathrm{ex}}^2}{2}\,\|\nabla \boldsymbol{m}_h^0\|_\omega^2 + k\sum_{i=0}^{j-1}\langle \boldsymbol{f}(t_{i+1/2}), \boldsymbol{v}_h^i\rangle_\omega + k\sum_{i=0}^{j-1}\langle (\boldsymbol{\pi}_h^i + \boldsymbol{\Pi}_h^i)(\boldsymbol{v}_h^i; \boldsymbol{m}_h^i, \boldsymbol{m}_h^{i-1}), \boldsymbol{v}_h^i\rangle_\omega \\
&\quad + \frac{1}{2}\,\|\boldsymbol{h}_h^0\|_\Omega^2 + k\sum_{i=0}^{j-1}\langle \boldsymbol{v}_h^i - \mathrm{d}_t \boldsymbol{m}_h^{i+1}, \boldsymbol{h}_h^{i+1/2}\rangle_\omega + k\sum_{i=0}^{j-1}\langle \boldsymbol{v}_h^i, \boldsymbol{h}_h^{i,\boldsymbol{\Theta}} - \boldsymbol{h}_h^{i+1/2}\rangle_\omega.
\end{aligned}$$

Recalling from (5.12) that $\|\mathrm{d}_t \boldsymbol{m}_h^{i+1}\|_\omega \lesssim \|\boldsymbol{v}_h^i\|_\omega$ we proceed as in the proof of Lemma 5.1(ii). Together with (2.15b) and (2.16b) the Young inequality proves that

$$\begin{aligned}
\chi_j &\lesssim \|\nabla \boldsymbol{m}_h^0\|_\omega^2 + \|\boldsymbol{h}_h^0\|_\Omega^2 + \frac{k}{\delta}\sum_{i=0}^{j-1}\|\boldsymbol{f}(t_{i+1/2})\|_\omega^2 + \frac{k}{\delta}\sum_{i=0}^{j-1}\|\boldsymbol{m}_h^i\|_\omega^2 + \frac{k}{\delta}\sum_{i=0}^{j-1}\|\nabla \boldsymbol{m}_h^i\|_\omega^2 \\
&\quad + \frac{k}{\delta}\sum_{i=0}^{j}\|\boldsymbol{h}_h^i\|_\omega^2 + \Big(\delta + k + \frac{k}{\delta\rho(k)}\Big)\,k\sum_{i=0}^{j-1}\|\boldsymbol{v}_h^i\|_\omega^2 + \delta k^2\rho(k)\sum_{i=0}^{j-1}\|\nabla \boldsymbol{v}_h^i\|_\omega^2.
\end{aligned} \tag{6.10}$$

Since $k/\rho(k) \to 0$ as $k \to 0$ we choose δ sufficiently small and can absorb $k\delta^{-1}\|\boldsymbol{h}_h^j\|_\omega^2 + k\sum_{i=0}^{j-1}\|\boldsymbol{v}_h^i\|_\omega^2 + \delta k^2\rho(k)\sum_{i=0}^{j-1}\|\nabla \boldsymbol{v}_h^i\|_\omega^2$ in χ_j. Altogether, we arrive at

$$\chi_j \lesssim 1 + k\sum_{i=0}^{j-1}\|\nabla \boldsymbol{m}_h^i\|_\omega^2 + k\sum_{i=0}^{j-1}\|\boldsymbol{h}_h^i\|_\Omega^2 \lesssim 1 + k\sum_{i=0}^{j-1}\chi_i.$$

Arguing as for Lemma 5.1(ii) we get that χ_j is uniformly bounded for all $j = 1, \dots, N$. In order to bound the remaining terms from (6.6) we sum (6.5) for $i = 0, \dots, j-1$ and multiply by k. Recall from (5.12)

that $\|\mathrm{d}_t \boldsymbol{m}_h^{i+1}\|_\omega \lesssim \|\boldsymbol{v}_h^i\|_\omega$. This yields

$$\mu_0 k \sum_{i=0}^{j-1} \|\mathrm{d}_t \boldsymbol{h}_h^{i+1}\|_\Omega^2 + \|\sigma^{-1/2}\nabla \times \boldsymbol{h}_h^j\|_\Omega^2 \overset{(6.5)}{\leq} \mu_0 k \sum_{i=0}^{j-1} \|\mathrm{d}_t \boldsymbol{m}_h^{i+1}\|_\omega^2 + \|\sigma^{-1/2}\nabla \times \boldsymbol{h}_h^0\|_\Omega^2$$
$$\lesssim k \sum_{i=0}^{j-1} \|\boldsymbol{v}_h^i\|_\omega^2 + \|\sigma^{-1/2}\nabla \times \boldsymbol{h}_h^0\|_\Omega^2 \overset{(6.10)}{\lesssim} \chi_j + \|\sigma^{-1/2}\nabla \times \boldsymbol{h}_h^0\|_\Omega^2.$$

Altogether, this proves (iii) and concludes the proof. □

LEMMA 6.2 Under the assumptions of Theorem 3.2(ii) consider the postprocessed output (2.5) of Algorithm 3.2. Then there exist $\boldsymbol{m} \in \boldsymbol{H}^1(\omega_T) \cap L^\infty(0,T;\boldsymbol{H}^1(\omega))$ and $\boldsymbol{h} \in H^1(0,T;\boldsymbol{L}^2(\Omega)) \cap L^\infty(0,T;\boldsymbol{H}(\mathrm{curl},\Omega))$ and a subsequence of each $\boldsymbol{m}_{hk}^\star \in \{\boldsymbol{m}_{hk}^=, \boldsymbol{m}_{hk}^-, \boldsymbol{m}_{hk}^+, \boldsymbol{m}_{hk}\}$, $\boldsymbol{h}_{hk}^\star \in \{\boldsymbol{h}_{hk}^=, \boldsymbol{h}_{hk}^-, \boldsymbol{h}_{hk}^+, \boldsymbol{h}_{hk}, \boldsymbol{h}_{hk}^{\boldsymbol{\Theta}}\}$, and of $\boldsymbol{v}_{hk}^-$ such that the convergence statements of Lemma 5.2(i)–(vii) for $\boldsymbol{m}_{hk}^\star$ and $\boldsymbol{v}_{hk}^-$ as well as the following (ix)–(xiii) for $\boldsymbol{h}_{hk}^\star$ hold true simultaneously for the same subsequence as $h,k \to 0$:

(ix) $\boldsymbol{h}_{hk} \rightharpoonup \boldsymbol{h}$ in $H^1(0,T;\boldsymbol{L}^2(\Omega))$,

(x) $\boldsymbol{h}_{hk}^\star \rightharpoonup \boldsymbol{h}$ in $\boldsymbol{L}^2(\Omega_T)$,

(xii) $\boldsymbol{h}_{hk}^\star \overset{*}{\rightharpoonup} \boldsymbol{h}$ in $L^\infty(0,T;\boldsymbol{H}(\mathrm{curl},\Omega))$,

(xii) $\boldsymbol{h}_{hk}^\star \rightharpoonup \boldsymbol{h}$ in $L^2(0,T;\boldsymbol{H}(\mathrm{curl},\Omega))$,

(xiii) $\boldsymbol{h}_{hk}^\star - \boldsymbol{h}_{hk} \to 0$ in $\boldsymbol{L}^2(\Omega_T)$.

Proof. Lemma 6.1(iii) yields uniform boundedness of $\boldsymbol{m}_{hk} \in \boldsymbol{H}^1(\omega_T)$, $\boldsymbol{m}_{hk}^\star \in L^\infty(0,T;\boldsymbol{H}^1(\omega))$, $\boldsymbol{h}_{hk} \in H^1(0,T;\boldsymbol{L}^2(\Omega))$ and $\boldsymbol{h}_{hk}^\star \in L^\infty(0,T;\boldsymbol{H}(\mathrm{curl},\Omega))$. The proofs of the convergence statements of Lemma 5.2(i)–(viii) and (ix)–(xi) follow as in Alouges (2008); Alouges *et al.* (2014) and Baňas *et al.* (2015); Le *et al.* (2015); Le & Tran (2013), respectively. Finally, (3.7) and Lemma 6.1(iii) prove that

$$\|\boldsymbol{h}_{hk} - \boldsymbol{h}_{hk}^\star\|_{\Omega_T}^2 \overset{(2.5)}{\lesssim} k^2 \sum_{i=0}^{N-1} \|\mathrm{d}_t \boldsymbol{h}_h^{i+1}\|_\Omega^2 \overset{(6.6)}{\lesssim} k \to 0 \quad \text{as } h,k \to 0.$$

This verifies Lemma 6.2 and concludes the proof. □

Proof of Theorem 3.2(ii). We prove that $(\boldsymbol{m},\boldsymbol{h})$ satisfies Definition 3.1(i)–(iv). Definition 3.1(i) follows as for LLG. Definition 3.1(ii) is an immediate consequence of Lemma 6.2(ix)–(xi). Definition 3.1(iii) follows as in Baňas *et al.* (2015); Le *et al.* (2015); Le & Tran (2013) from Lemma 6.2(i) and (ix).

It remains to verify Definition 3.1: To that end adopt the notation of the proof of Theorem 2.2(ii). In addition let $\mathscr{J}_h : \boldsymbol{H}(\mathbf{curl};\Omega) \to \mathscr{X}_h$ denote the interpolation operator for first-order Nédélec elements of second type; see Nédélec (1986). Let $\boldsymbol{\varphi} \in \boldsymbol{C}^\infty(\overline{\omega_T})$, $\boldsymbol{\zeta} \in \boldsymbol{C}^\infty(\overline{\Omega_T})$ and $t \in [0,T]$. For $t \in [t_i, t_{i+1})$ and

$i = 0, \dots, N-1$ we test (3.5) with $\mathscr{I}_h(\boldsymbol{m}_h^i \times \boldsymbol{\varphi}(t)) \in \mathscr{K}_h(\boldsymbol{m}_h^i)$ and $\mathscr{J}_h(\boldsymbol{\zeta}(t)) \in \mathscr{X}_h$ and integrate over $(0,T)$. With the definition of the postprocessed output (2.5), we obtain

$$
\begin{aligned}
&I_{hk}^1 + I_{hk}^2 + \frac{\ell_{\mathrm{ex}}^2}{2} I_{hk}^3 \\
&=: \int_0^T \langle W_{M(k)}(\lambda_{hk}^-)\boldsymbol{v}_{hk}^-, \mathscr{I}_h(\boldsymbol{m}_{hk}^- \times \boldsymbol{\varphi})\rangle_\omega \,\mathrm{d}t + \int_0^T \langle \boldsymbol{m}_{hk}^- \times \boldsymbol{v}_{hk}^-, \mathscr{I}_h(\boldsymbol{m}_{hk}^- \times \boldsymbol{\varphi})\rangle_\omega \,\mathrm{d}t \\
&\quad + \frac{\ell_{\mathrm{ex}}^2}{2} k\,(1+\rho(k)) \int_0^T \langle \nabla \boldsymbol{v}_{hk}^-, \nabla \mathscr{I}_h(\boldsymbol{m}_{hk}^- \times \boldsymbol{\varphi})\rangle_\omega \,\mathrm{d}t \\
&\overset{(3.5a)}{=} -\ell_{\mathrm{ex}}^2 \int_0^T \langle \nabla \boldsymbol{m}_{hk}^-, \nabla \mathscr{I}_h(\boldsymbol{m}_{hk}^- \times \boldsymbol{\varphi})\rangle_\omega \,\mathrm{d}t + \int_0^T \langle \boldsymbol{\pi}_{hk}^-(\boldsymbol{v}_{hk}^-; \boldsymbol{m}_{hk}^-, \boldsymbol{m}_{hk}^{=}), \mathscr{I}_h(\boldsymbol{m}_{hk}^- \times \boldsymbol{\varphi})\rangle_\omega \,\mathrm{d}t \\
&\quad + \int_0^T \langle \bar{\boldsymbol{f}}_k, \mathscr{I}_h(\boldsymbol{m}_{hk}^- \times \boldsymbol{\varphi})\rangle_\omega \,\mathrm{d}t + \int_0^T \langle \boldsymbol{\Pi}_{hk}^-(\boldsymbol{v}_{hk}^-; \boldsymbol{m}_{hk}^-, \boldsymbol{m}_{hk}^{=}), \mathscr{I}_h(\boldsymbol{m}_{hk}^- \times \boldsymbol{\varphi})\rangle_\omega \,\mathrm{d}t \\
&\quad + \int_0^T \langle \boldsymbol{h}_{hk}^{\boldsymbol{\Theta}}, \mathscr{I}_h(\boldsymbol{m}_{hk}^- \times \boldsymbol{\varphi})\rangle_\omega \,\mathrm{d}t =: -\ell_{\mathrm{ex}}^2 I_{hk}^4 + I_{hk}^5 + I_{hk}^6 + I_{hk}^7 + I_{hk}^8,
\end{aligned} \tag{6.11a}
$$

and

$$
\begin{aligned}
&-\mu_0 I_{hk}^9 := -\mu_0 \int_0^T \langle \partial_t \boldsymbol{m}_{hk}, \mathscr{J}_h \boldsymbol{\zeta}\rangle_\omega \,\mathrm{d}t \\
&\overset{(3.5b)}{=} \mu_0 \int_0^T \langle \partial_t \boldsymbol{h}_{hk}, \mathscr{J}_h \boldsymbol{\zeta}\rangle_\Omega \,\mathrm{d}t + \int_0^T \langle \sigma^{-1}\nabla \times \overline{\boldsymbol{h}}_{hk}, \nabla \times (\mathscr{J}_h \boldsymbol{\zeta})\rangle_\Omega \,\mathrm{d}t =: \mu_0 I_{hk}^{10} + I_{hk}^{11}.
\end{aligned} \tag{6.11b}
$$

With Lemma 6.2, convergence of the integrals $I_{hk}^1, \dots, I_{hk}^7$ in (6.11a) towards their continuous counterparts in the variational formulation (3.3) follows the lines of the proof of Theorem 2.2(ii). Thus, we only consider the integrals $I_{hk}^8, \dots, I_{hk}^{11}$ from (6.11): as in Le *et al.* (2015); Le & Tran (2013), we get from Lemma 6.2 and the convergence properties of $\mathscr{I}_h$ and $\mathscr{J}_h$ that

$$
I_{hk}^{10} \to \int_0^T \langle \partial_t \boldsymbol{h}, \boldsymbol{\zeta}\rangle_\Omega \,\mathrm{d}t \quad \text{as } h, k \to 0.
$$

For the remaining terms, Lemma 6.2 and the convergence properties of $\mathscr{J}_h$ yield

$$
I_{hk}^9 \to \int_0^T \langle \partial_t \boldsymbol{m}, \boldsymbol{\zeta}\rangle_\omega \,\mathrm{d}t, \quad I_{hk}^8 \to \int_0^T \langle \boldsymbol{h}, \boldsymbol{m} \times \boldsymbol{\varphi}\rangle_\omega \,\mathrm{d}t, \quad I_{hk}^{11} \to \int_0^T \langle \sigma^{-1}\nabla \times \boldsymbol{h}, \nabla \times \boldsymbol{\zeta}\rangle_\Omega \,\mathrm{d}t
$$

as $h, k \to 0$. This concludes the proof. □

Proof of Theorem 3.2(iii). It remains to verify that $(\boldsymbol{m}, \boldsymbol{h})$ from Lemma 6.2 satisfies Definition 3.1(v). To that end let $\tau \in (0,T)$ be arbitrary. With the stronger assumptions on $\boldsymbol{\pi}$ and $\boldsymbol{f}$ from (2.17) we argue

as in the proof of Theorem 2.3(iii) to see that

$$\begin{aligned}
&\mathscr{E}_{\mathrm{ELLG}}(\boldsymbol{m}_{hk}^{+}(\tau),\boldsymbol{h}_{hk}^{+}(\tau)) - \mathscr{E}_{\mathrm{ELLG}}(\boldsymbol{m}_{h}^{0},\boldsymbol{h}_{h}^{0}) + \int_0^{t_j} \langle W_{M(k)}(\boldsymbol{m}_{hk}^{-})\boldsymbol{v}_{hk}^{-},\boldsymbol{v}_{hk}^{-}\rangle_{\omega}\,\mathrm{d}t \\
&\quad + \int_0^{t_j} \langle \partial_t \boldsymbol{f}_k,\boldsymbol{m}_{hk}^{-}\rangle_{\omega}\,\mathrm{d}t - \int_0^{t_j} \langle \boldsymbol{\Pi}_{hk}(\boldsymbol{v}_{hk}^{-};\boldsymbol{m}_{hk}^{-},\boldsymbol{m}_{hk}^{=}),\boldsymbol{v}_{hk}^{-}\rangle_{\omega}\,\mathrm{d}t \\
&\lesssim k\int_0^{t_j} \|\boldsymbol{v}_{hk}^{-}\|_{\Omega}^2\,\mathrm{d}t + k\int_0^{t_j} \|\boldsymbol{v}_{hk}^{-}\|_{\Omega}\|\nabla\boldsymbol{v}_{hk}^{-}\|_{\Omega}\,\mathrm{d}t \\
&\quad + \int_0^{t_j} |\langle \boldsymbol{\pi}_{hk}(\boldsymbol{v}_{hk}^{-};\boldsymbol{m}_{hk}^{-},\boldsymbol{m}_{hk}^{=}) - \boldsymbol{\pi}(\boldsymbol{m}_{hk}^{-}),\boldsymbol{v}_{hk}^{-}\rangle_{\omega}|\,\mathrm{d}t + \int_0^{t_j} |\langle \overline{\boldsymbol{f}}_k - \boldsymbol{f},\boldsymbol{v}_{hk}^{-}\rangle_{\omega}|\,\mathrm{d}t \\
&\quad + \int_0^{t_j} |\langle \boldsymbol{h}_{hk}^{\boldsymbol{\Theta}} - \overline{\boldsymbol{h}}_{hk},\boldsymbol{v}_{hk}^{-}\rangle_{\omega}|\,\mathrm{d}t + \int_0^{t_j} |\langle \overline{\boldsymbol{h}}_{hk},\boldsymbol{v}_{hk}^{-} - \partial_t\boldsymbol{m}_{hk}\rangle_{\omega}|\,\mathrm{d}t\,. \qquad (6.12)
\end{aligned}$$

The only crucial term is the last one on the right-hand side of (6.12): according to the Riesz–Thorin theorem, the Sobolev embedding $H^1(\omega)\subset L^6(\omega)$ and an inverse estimate,

$$\|v_h\|_{L^4(\omega)} \le \|v_h\|_{L^2(\omega)}^{1/4}\|v_h\|_{L^6(\omega)}^{3/4} \lesssim \|v_h\|_{L^2(\omega)}^{1/4}\|v_h\|_{H^1(\omega)}^{3/4} \lesssim h^{-3/4}\|v_h\|_{L^2(\omega)} \quad \text{for all} v_h \in V_h.$$

Together with Lemma 6.1(iii) this yields

$$\begin{aligned}
\int_0^{t_j} |\langle \overline{\boldsymbol{h}}_{hk},\boldsymbol{v}_{hk}^{-} - \partial_t\boldsymbol{m}_{hk}\rangle_{\omega}|\,\mathrm{d}t &\le \|\overline{\boldsymbol{h}}_{hk}\|_{L^\infty(0,T;\boldsymbol{L}^2(\Omega))}\|\boldsymbol{v}_{hk}^{-} - \partial_t\boldsymbol{m}_{hk}\|_{L^1(0,T;\boldsymbol{L}^2(\omega))} \\
&\overset{(5.12)}{\lesssim} k\|\boldsymbol{v}_{hk}^{-}\|_{L^2(0,T;\boldsymbol{L}^4(\omega))}^2 \lesssim kh^{-3/2}\,\|\boldsymbol{v}_{hk}^{-}\|_{\boldsymbol{L}^2(\omega_T)}^2 \longrightarrow 0
\end{aligned} \qquad (6.13)$$

as $h,k\to 0$, where we have used an inverse inequality and the assumption $k=\mathbf{o}(h^{3/2})$. Arguing by lower semicontinuity we conclude the proof as for Theorem 3.3. □

7. Numerical experiments

This section provides some numerical experiments for Algorithms 2.2 and 3.2. The computations have been performed with our micromagnetic software Commics (see Pfeiler *et al.*, 2018), based on the open-source finite element library Netgen/NGSolve (see Schöberl, 2017). The computation of the stray field $\boldsymbol{h}_{\mathrm{s}} = -\nabla u$ requires the approximation of the magnetostatic potential $u\in H^1(\mathbb{R}^3)$, which solves the full space transmission problem

$$-\Delta u = -\operatorname{div}\boldsymbol{m} \qquad \text{in } \omega, \qquad (7.1a)$$

$$-\Delta u = 0 \qquad \text{in } \mathbb{R}^3\setminus\overline{\omega}, \qquad (7.1b)$$

$$u^{\mathrm{ext}} - u^{\mathrm{int}} = 0 \qquad \text{on } \partial\omega, \qquad (7.1c)$$

$$(\nabla u^{\mathrm{ext}} - \nabla u^{\mathrm{int}})\cdot\boldsymbol{n} = -\boldsymbol{m}\cdot\boldsymbol{n} \qquad \text{on } \partial\omega, \qquad (7.1d)$$

$$u(\boldsymbol{x}) = \mathscr{O}(|\boldsymbol{x}|^{-1}) \qquad \text{as } |\boldsymbol{x}|\to\infty. \qquad (7.1e)$$

Here, the superscript *ext* (resp. *int*) refers to the traces of u on $\partial\omega$ with respect to the exterior domain $\mathbb{R}^3 \setminus \overline{\omega}$ (resp. the interior domain ω), and $\boldsymbol{n}$ is the outer normal vector on $\partial\omega$. Recall from Praetorius (2004) that $\boldsymbol{\pi}(\boldsymbol{m}) := -\nabla u$ gives rise to a self-adjoint operator $\boldsymbol{\pi} \in L(\boldsymbol{L}^2(\omega), \boldsymbol{L}^2(\mathbb{R}^3))$, which also satisfies the stronger stability assumption (2.17).

To discretize (7.1) we employ the hybrid FEM-BEM method from Fredkin & Koehler (1990). We note that the latter satisfies (2.15) with strong convergence in (2.15c); see Bruckner *et al.* (2014, Section 4.4.1) or Praetorius *et al.* (2018, Section 4.1) for details. This part of the code builds upon the open-source Galerkin boundary element library BEM++ (Śmigaj *et al.*, 2015). The arising linear systems are solved with GMRES (resp. with CG for the hybrid FEM-BEM approach) with tolerance 10^{-12}.

7.1 *Empirical convergence rates for LLG*

We aim to illustrate the accuracy and the computational effort of Algorithm 2.2. We compare the following strategies for the lower-order terms:

- `TPS2`: fully implicit approach proposed in Alouges *et al.* (2014) and described in Remark 2.1(iii);
- `TPS2+AB`: Adams–Bashforth approach proposed in this work and described in Remark 2.1(iv);
- `TPS2+EE`: explicit Euler approach, where $\boldsymbol{\pi}_h^i(\boldsymbol{v}_h^i; \boldsymbol{m}_h^i, \boldsymbol{m}_h^{i-1}) := \boldsymbol{\pi}_h(\boldsymbol{m}_h^i)$.

For all strategies we employ the canonical choices (2.7) for M and ρ. For `TPS2`, where $\boldsymbol{\pi}_h^i$ and $\boldsymbol{\Pi}_h^i$ effectively depend on $\boldsymbol{v}_h^i$ (see (2.12)), the linear system (2.10) of Algorithm 2.2 is solved with the fixed-point iteration used in the proof of Theorem 2.2(i), which is stopped when $\|\boldsymbol{\eta}_h^\ell - \boldsymbol{\eta}_h^{\ell-1}\|_{\boldsymbol{L}^2(\omega)} \leq 10^{-10}$. In addition we consider the original (first-order) tangent plane scheme of Alouges (2008) with $\theta = 1/2$ (i.e., formal Crank–Nicolson-type integrator, which can be seen as a special case of Algorithm 2.2 with $W_{M(k)} \equiv \alpha$ and $\rho \equiv 0$) together with the following two strategies for the integration of the lower-order terms:

- `TPS1+AB`: Adams–Bashforth approach (2.13);
- `TPS1+EE`: explicit Euler approach analyzed in Alouges *et al.* (2012); Bruckner *et al.* (2014).

To test the schemes we use the model problem proposed in Praetorius *et al.* (2018): we consider the initial boundary value problem (2.1) with $\omega = (0,1)^3$, $\boldsymbol{m}^0 \equiv (1,0,0)$, $\alpha = 1$ and $T = 5$. For the effective field (2.1d) we choose $\ell_{\text{ex}} = 1$, a constant field $\boldsymbol{f} \equiv (-2, -0.5, 0)$, as well as an operator $\boldsymbol{\pi}$, which only involves the stray field, i.e., $\boldsymbol{\pi}(\boldsymbol{m}) = -\nabla u$; see (7.1).

We consider a fixed triangulation $\mathcal{T}_h$ of ω generated by Netgen, which consists of 3939 elements and 917 nodes (prescribed mesh size $h = 1/8$). The exact solution is unknown. To compute the empirical convergence rates we consider a reference solution $\boldsymbol{m}_{hk_{\text{ref}}}$ computed with `TPS2`, using the above mesh and the time step size $k_{\text{ref}} = 5 \cdot 10^{-5}$. Table 1 gives the average computational time per time step for each of the considered five integrators. In Fig. 1a we plot the cumulative computational costs for the integration up to the final time T. We observe a vast improvement if the lower-order terms (i.e., the stray field) are integrated explicitly in time. The extended (first-order) tangent plane scheme from Alouges (2008) leads to the cheapest costs, since Algorithm 2.2 involves additional computations in each time step for λ_h^i as well as the weighted mass matrix corresponding to $\langle W_{M(k)}(\lambda_h^i)\,\cdot, \cdot\rangle_\omega$.

Figure 1b visualizes the experimental convergence order of the five integrators. As expected `TPS2` and `TPS+AB` lead to second-order convergence in time. Essentially, both integrators even lead quantitatively to the same accuracy of the numerical solution. `TPS2+EE`, as well as `TPS1+EE`, yields

TABLE 1 *Experiment of Section 7.1: average computational time for one time step of the different integrators, where we provide the absolute time (in seconds) for the algorithm (`TPS2`) from Alouges et al. (2014) as well as the relative times of all other integrators*

	`TPS2` absolute	`TPS2` relative	`TPS1+EE` relative	`TPS1+AB` relative	`TPS2+EE` relative	`TPS2+AB` relative
$k = 0.0016$	0.12	100%	30.14%	33.96%	41.53%	47.08%
$k = 0.0008$	0.12	100%	30.04%	35.81%	41.51%	45.61%
$k = 0.0004$	0.12	100%	30.15%	33.90%	41.61%	45.36%
$k = 0.0002$	0.12	100%	30.43%	36.10%	41.81%	45.85%
$k = 0.0001$	0.11	100%	32.39%	36.52%	44.68%	48.96%

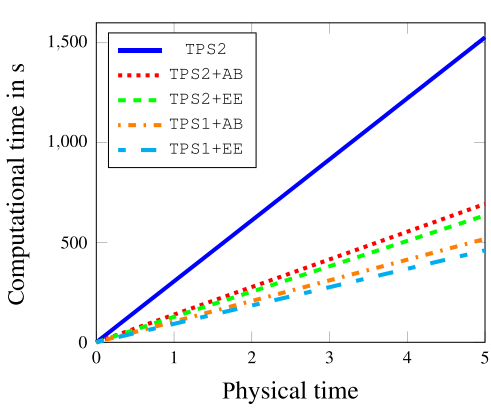

(a) Cumulative computational time for $k = 4 \cdot 10^{-4}$.

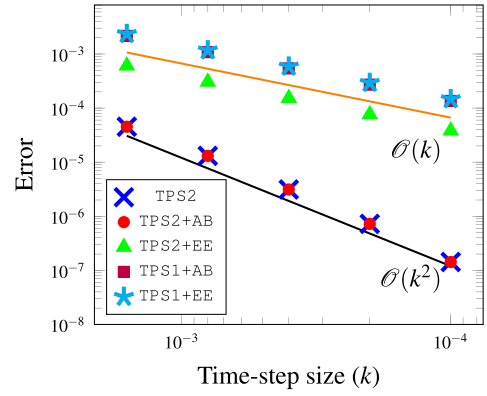

(b) Reference error $\max_j \|\boldsymbol{m}_{hk_{\text{ref}}}(t_j) - \boldsymbol{m}_{hk}(t_j)\|_{\boldsymbol{H}^1(\omega)}$ for $k = 2^\ell k_{\text{ref}}$ with $\ell \in \{1,2,3,4,5\}$ and $k_{\text{ref}} = 5 \cdot 10^{-5}$.

FIG. 1. Experiments of Section 7.1: cumulative computational time (left) and convergence order (right) of the different integrators.

first-order convergence, since the explicit Euler integration of the stray field is only first-order accurate. Differently from the classical θ-method for linear second-order parabolic PDEs, due to the presence of the nodal projection, the original tangent plane scheme (Alouges, 2008) with $\theta = 1/2$ (Crank–Nicolson-type `TPS1+AB`) does not lead to any improvement of the convergence order in time (from first-order to second-order).

Overall, the proposed `TPS2+AB` integrator appears to be the method of choice with respect to both computational time and empirical accuracy.

7.2 *Spintronic extensions of LLG*

We consider two spintronic extensions of LLG, where the energy-based effective field is supplemented by terms that model the effect of the so-called spin transfer torque (STT) (Berger, 1996; Slonczewski, 1996), and perform physically relevant numerical experiments with the integrator `TPS2+AB`; see Section 7.1.

7.2.1 *Slonczewski model.* Since the discovery of the GMR effect (Baibich *et al.*, 1988; Binasch *et al.*, 1989) magnetic multilayers, i.e., systems consisting of alternating ferromagnetic and nonmagnetic

sublayers, have become the subject of intense research in metal spintronics. A phenomenological model to include the STT in magnetic multilayers with current-perpendicular-to-plane injection geometry was proposed in Slonczewski (1996). This model is covered by our framework for LLG (2.1) by considering

$$\boldsymbol{\Pi} : \boldsymbol{L}^\infty(\omega) \to \boldsymbol{L}^2(\omega), \quad \boldsymbol{\Pi}(\boldsymbol{\varphi}) := G(\boldsymbol{\varphi} \cdot \boldsymbol{p})\, \boldsymbol{\varphi} \times \boldsymbol{p}, \tag{7.2a}$$

where $\boldsymbol{p} \in \mathbb{R}^3$ with $|\boldsymbol{p}| = 1$ is constant, while the function $G : [-1, 1] \to \mathbb{R}$ belongs to $C^1([-1, 1])$. Using the chain rule and the product rule we obtain

$$\partial_t \boldsymbol{\Pi}(\boldsymbol{\varphi}) = G'(\boldsymbol{\varphi} \cdot \boldsymbol{p})(\partial_t \boldsymbol{\varphi} \cdot \boldsymbol{p})\, \boldsymbol{\varphi} \times \boldsymbol{p} + G(\boldsymbol{\varphi} \cdot \boldsymbol{p})\, \partial_t \boldsymbol{\varphi} \times \boldsymbol{p}.$$

Hence, we recover the framework of Section 2.4 if we consider the operator

$$\boldsymbol{D}(\boldsymbol{\varphi}, \boldsymbol{\psi}) = G'(\boldsymbol{\varphi} \cdot \boldsymbol{p})(\boldsymbol{\psi} \cdot \boldsymbol{p})\, \boldsymbol{\varphi} \times \boldsymbol{p} + G(\boldsymbol{\varphi} \cdot \boldsymbol{p})\, \boldsymbol{\psi} \times \boldsymbol{p} \tag{7.2b}$$

as well as the 'discrete' operators

$$\boldsymbol{\Pi}_h(\boldsymbol{\varphi}) = \boldsymbol{\Pi}(\boldsymbol{\varphi}) \quad \text{and} \quad \boldsymbol{D}_h(\boldsymbol{\varphi}, \boldsymbol{\psi}) = \boldsymbol{D}(\boldsymbol{\varphi}, \boldsymbol{\psi}); \tag{7.2c}$$

see Remark 2.1(iii). The resulting approximate operators $\boldsymbol{\Pi}_h^i$, and the piecewise constant time reconstruction $\boldsymbol{\Pi}_{hk}^-$, satisfy the assumptions (2.16) of Theorem 2.2; see Di Fratta *et al.* (2017, Section 7.2.1) for the verification.

To test our algorithm we simulate the writing process of an STT random access memory (Hosomi *et al.*, 2005) and reproduce the switching of a ferromagnetic film without external field. The computational domain is an elliptic cylinder of height $d = 10$ nm (aligned with the z-direction) and elliptic cross section with semiaxis lengths $a = 60$ nm and $b = 35$ nm (parallel to the x–y plane);

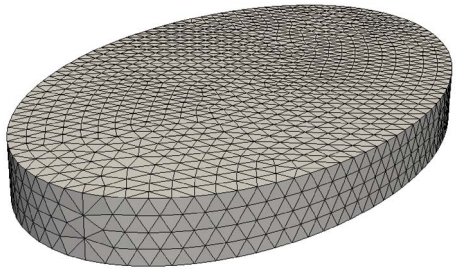

(a) Computational domain.

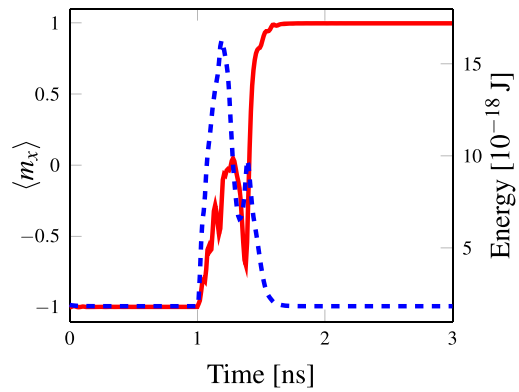

(b) Time evolutions of $\langle m_x \rangle$ (red solid line, left scale) and of the total energy (blue dashed line, right scale) during the switching process.

FIG. 2. Experiment of Section 7.2.1: current-induced switching of a ferromagnetic film.

see Fig. 2a. The film is supposed to be the free layer of a magnetic trilayer, which also includes a second ferromagnetic layer (the so-called fixed layer) with constant uniform magnetization $\boldsymbol{p} = (1, 0, 0)$ and a conducting nonmagnetic spacer. For the material parameters we choose the values of permalloy: damping parameter $\alpha = 0.1$, saturation magnetization $M_s = 8.0 \cdot 10^5$ A/m, exchange stiffness constant $A = 1.3 \cdot 10^{-11}$ J/m, uniaxial anisotropy with constant $K = 5.0 \cdot 10^2$ J/m^3 and easy axis $\boldsymbol{a} = (1, 0, 0)$. With these choices the effective field takes the form (2.1d) with

$$\ell_{\text{ex}} = \sqrt{\frac{2A}{\mu_0 M_s^2}} \approx 5.7\,\text{nm}, \quad \boldsymbol{\pi}(\boldsymbol{m}) = \frac{2K}{\mu_0 M_s^2}(\boldsymbol{a} \cdot \boldsymbol{m})\boldsymbol{a} - \nabla u \quad \text{and} \quad \boldsymbol{f} \equiv \boldsymbol{0}, \tag{7.3}$$

where $\mu_0 = 4\pi \cdot 10^{-7}$ N/A^2 is the vacuum permeability and u is the magnetostatic potential, solution of the transmission problem (7.1).

Starting from the uniform initial configuration $\boldsymbol{m}^0 \equiv (-1, 0, 0)$ we solve (2.1) with $\boldsymbol{\Pi} \equiv \boldsymbol{0}$ for 1ns to reach a relaxed state. Then we inject a spin-polarized electric current with intensity $J_e = 1 \cdot 10^{12}$ A/m^2 for 1ns. The resulting STT is modeled by the operator (7.2a), where the function G takes the phenomenological expression

$$G(x) = \frac{\hbar J_e}{e\mu_0 M_s^2 d}\left[\frac{(1+P)^3(3+x)}{4P^{3/2}} - 4\right]^{-1} \quad \text{for all } x \in [-1, 1];$$

see Slonczewski (1996). Here, $\hbar = 1.054571800 \cdot 10^{-34}$ Js denotes the reduced Planck constant, $e = 1.602176621 \cdot 10^{-19}$ C denotes the elementary charge, while $P = 0.8$ is the polarization parameter. We solve (2.1) with $\boldsymbol{\Pi} \equiv \boldsymbol{0}$ for 1ns to relax the system to the new equilibrium.

For the spatial discretization we consider a tetrahedral triangulation with prescribed mesh size 3 nm (15 885 elements, 3 821 nodes) generated by Netgen. For the time discretization we consider a constant time step size of 0.1ps (30 000 time steps).

The time evolutions of the average x-component $\langle m_x \rangle$ of the magnetization in the free layer and of the total energy (2.2) are depicted in Fig. 2b Since the size of the film is well under the single-domain limit (see, e.g., Alouges *et al.*, 2015) the initial uniform magnetization configuration is preserved by the first relaxation process. By applying a perpendicular spin-polarized current, the uniform magnetization of the free layer can be switched from $(-1, 0, 0)$ to $\boldsymbol{p} = (1, 0, 0)$. The fundamental physics underlying this phenomenon is understood as the mutual transfer of spin angular momentum between the $\boldsymbol{p}$-polarized conduction electrons and the magnetization of the film. During the switching process, the classical energy dissipation modulated by the damping parameter α is lost as an effect of the Slonczewski contribution; see the fourth term on the left-hand side of (2.4). The new state is also stable and is preserved by the final relaxation process.

7.2.2 *Zhang–Li model.* In Zhang & Li (2004) the authors derived an extended form of LLG to model the effect of an electric current flow on the magnetization dynamics in single-phase samples characterized by a current-in-plane injection geometry. A similar equation was obtained in a phenomenological way in Thiaville *et al.* (2005) for the description of the current-driven motion of domain walls in patterned nanowires. Here, the operator takes the form

$$\boldsymbol{\Pi} : \boldsymbol{H}^1(\omega) \cap \boldsymbol{L}^\infty(\omega) \to \boldsymbol{L}^2(\omega), \quad \boldsymbol{\Pi}(\boldsymbol{\varphi}) := \boldsymbol{\varphi} \times (\boldsymbol{u} \cdot \nabla)\boldsymbol{\varphi} + \beta(\boldsymbol{u} \cdot \nabla)\boldsymbol{\varphi}, \tag{7.4a}$$

where $\boldsymbol{u} \in \boldsymbol{L}^\infty(\omega)$ and $\beta > 0$ is constant. The product rule yields

$$\partial_t \boldsymbol{\Pi}(\boldsymbol{\varphi}) = \partial_t \boldsymbol{\varphi} \times (\boldsymbol{u} \cdot \nabla)\boldsymbol{\varphi} + \boldsymbol{\varphi} \times (\boldsymbol{u} \cdot \nabla)\partial_t \boldsymbol{\varphi} + \beta(\boldsymbol{u} \cdot \nabla)\partial_t \boldsymbol{\varphi}.$$

Hence, we recover the framework of Section 2.4 if we consider the operators

$$\boldsymbol{D}(\boldsymbol{\varphi}, \boldsymbol{\psi}) = \boldsymbol{\psi} \times (\boldsymbol{u} \cdot \nabla)\boldsymbol{\varphi} + \boldsymbol{\varphi} \times (\boldsymbol{u} \cdot \nabla)\boldsymbol{\psi} + \beta(\boldsymbol{u} \cdot \nabla)\boldsymbol{\psi}, \tag{7.4b}$$

$$\boldsymbol{\Pi}_h(\boldsymbol{\varphi}) = \boldsymbol{\Pi}(\boldsymbol{\varphi}) \quad \text{and} \quad \boldsymbol{D}_h(\boldsymbol{\varphi}, \boldsymbol{\psi}) = \boldsymbol{D}(\boldsymbol{\varphi}, \boldsymbol{\psi}). \tag{7.4c}$$

In Di Fratta *et al.* (2017, Section 7.2.2) we prove that Theorem 2.2(i)–(ii) with the Adams–Bashforth approach from Remark 2.1(iv) still holds if we additionally suppose

$$\sup_{h>0} \|\nabla \boldsymbol{m}_h^0\|_{\boldsymbol{L}^\infty(\omega)} \leq C.$$

The extended LLG forms of Zhang & Li (2004); Thiaville *et al.* (2005) are the subject of the μMAG standard problem #5, proposed by the Micromagnetic Modeling Activity Group of the National Institute of Standards and Technology (see NIST Micromagnetic Modeling Activity Group (2014)). The sample under consideration is a permalloy film with dimensions 100 nm × 100 nm × 10 nm, aligned with the x-, y- and z-axes of a Cartesian coordinate system, with origin at the center of the film. For the material parameters, we consider the same values as in Section 7.2.1,

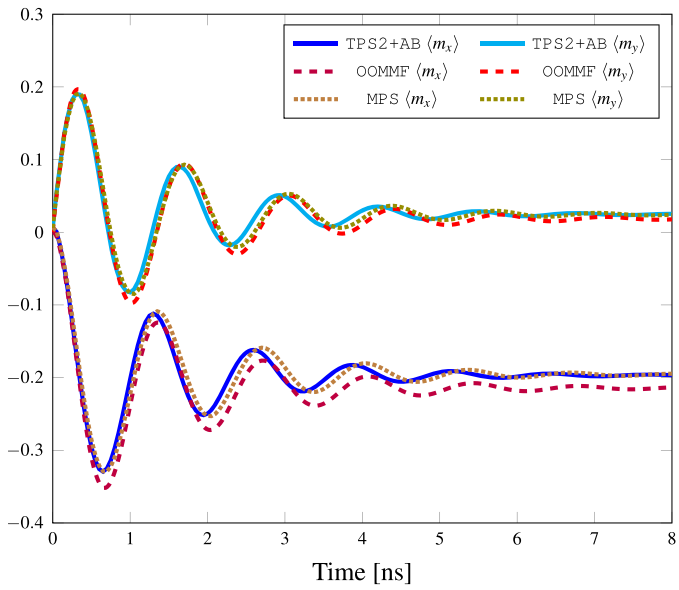

(a) Time evolutions of $\langle m_x \rangle$ and $\langle m_y \rangle$.

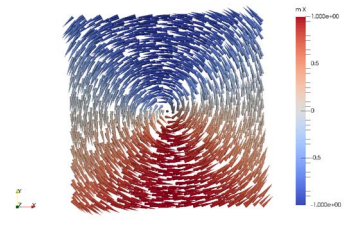

(b) Initial vortex state.

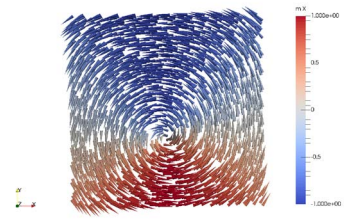

(c) Final vortex state.

FIG. 3. Experiment of Section 7.2.2: comparison of the results obtained for μMAG standard problem #5 with TPS2+AB, OOMMF and MPS.

except for the magnetocrystalline anisotropy, which is neglected, i.e., $K = 0$. The initial state is obtained by solving (2.1) for the initial condition $\boldsymbol{m}^0(x,y,z) = (-y,x,R)/\sqrt{x^2+y^2+R^2}$ with R=10 nm and $\boldsymbol{\Pi} \equiv \mathbf{0}$ for a sufficiently long time, until the system relaxes to equilibrium; see Fig. 3b. Given the spin velocity vector $\boldsymbol{u}_T = (-72.17, 0, 0)$ m/s and the gyromagnetic ratio $\gamma_0 = 2.21 \cdot 10^5$ m/(As) we define $\boldsymbol{\Pi}$ by (7.4a) for $\boldsymbol{u} = -\boldsymbol{u}_T/(\gamma_0 M_s)$ and $\beta = 0.05$. With the relaxed magnetization configuration as initial condition we solve (2.1) for 8 ns, which turns out to be a sufficiently long time to reach the new equilibrium; see Fig. 3c.

For the simulation we consider a tetrahedral triangulation of the domain into 25 666 elements with prescribed maximal diameter 3 nm (5 915 nodes) generated by Netgen. For the time discretization, we consider a constant time-step size of 0.1 ps (80 000 *uniform* time steps).

We compare our results with those obtained with the finite difference code `OOMMF` (Donahue & Porter, 1999) and with the implicit–explicit midpoint scheme of Praetorius *et al.* (2018) (`MPS`). For `OOMMF` we consider the data downloadable from the μMAG homepage (see NIST Micromagnetic Modeling Activity Group 2014), which refer to a uniform partition of the computational domain into 12 500 cubes with 2 nm edge and 42 350 *adaptive* time steps. In `OOMMF` the solution of (7.1) for the stray field computation is based on a fast Fourier transform algorithm. The results for `MPS` refer to the same triangulation used for `TPS2+AB`, but are obtained with a 20 times smaller time-step size (5 fs, i.e., 1600 000 time steps), which is necessary to ensure the well-posedness of the fixed-point iteration that solves the nonlinear system (Praetorius *et al.*, 2018). Figure 3a shows the evolution of the averages $\langle m_x \rangle$ and $\langle m_y \rangle$ of the x- and y-components of $\boldsymbol{m}$, respectively. Despite the different nature of the methods the results are in full qualitative agreement.

7.3 *Empirical convergence rates for ELLG*

We aim to illustrate the accuracy and the computational effort of Algorithm 3.2. We compare the following four strategies:

- `FC-2`: the fully coupled nonlinear implicit approach described in Remark 3.1(iii);
- `DC-2`: the decoupled linear explicit Adams–Bashforth approach described in Remark 3.1(iv);
- `DC-1`: a decoupled linear explicit Euler approach, i.e., $\boldsymbol{h}_h^{i,\boldsymbol{\Theta}} = \boldsymbol{h}_h^i$ for all $i = 0, \dots, N-1$;
- `FC-1`: the fully coupled linear implicit approach described in Remark 3.1(v).

We always employ the canonical choices (2.7) for M and ρ. For all time steps of `FC-2` we solve the nonlinear system (3.5) by the fixed-point iteration from the proof of Theorem 3.2(i), which we stop if $\|\boldsymbol{\eta}_h^\ell - \boldsymbol{\eta}_h^{\ell-1}\|_\omega + \|\boldsymbol{v}_h^\ell - \boldsymbol{v}_h^{\ell-1}\|_\Omega \le 10^{-10}$.

To test the schemes we choose $\omega = (-0.125, 0.125)^3$, $\Omega = (-1,1)^3$ and $T = 7$. For the LLG part (3.1a), we choose $\alpha = 1$, $\ell_{\mathrm{ex}}^2 = 1$, $\boldsymbol{\pi} = \boldsymbol{\Pi} = \mathbf{0}$, and set $\boldsymbol{f} = (f_1, 0, 0)^{\mathrm{T}} \in \boldsymbol{C}^1([0,T])$, where

$$f_1(t) := \begin{cases} 15t^2 & \text{for } 0 \le t \le 1, \\ 30 - 15(t-2)^2 & \text{for } 1 < t \le 2, \\ 30 & \text{for } 2 < t \le 4, \\ 30 - 15(t-4)^2 & \text{for } 4 < t \le 5, \\ 15(t-6)^2 & \text{for } 5 < t \le 6, \\ 0 & \text{for } 6 < t \le 7. \end{cases}$$

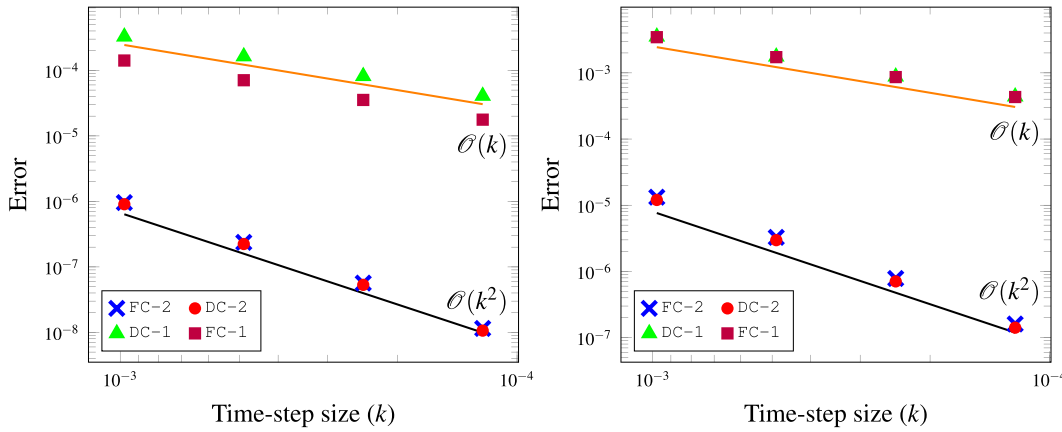

FIG. 4. Experiment of Section 7.3: reference error $\max_j(\|\boldsymbol{m}_{hk_{\mathrm{ref}}}(t_j) - \boldsymbol{m}_{hk}(t_j)\|_{\boldsymbol{H}^1(\omega)})$ (left) and $\max_j(\|\boldsymbol{h}_{hk_{\mathrm{ref}}}(t_j) - \boldsymbol{h}_{hk}(t_j)\|_{\boldsymbol{H}(\mathbf{curl};\Omega)})$ (right) for $k = 2^\ell k_{\mathrm{ref}}$ with $\ell \in \{1,2,3,4\}$ and $k_{\mathrm{ref}} = 2^{-14}$.

For the eddy current part (3.1b), let $\mu_0 = 1$, and $\sigma \in L^\infty(\Omega)$ with $\sigma|_\omega = 100$ and $\sigma|_{\Omega\setminus\overline{\omega}} = 1$. We use a fixed triangulation $\mathscr{T}_h$ of Ω generated by Netgen, which resolves ω with prescribed maximum mesh sizes $h_{\mathrm{in}} = 0.03$ on the submesh $\mathscr{T}_h|_\omega$, and $h_{\mathrm{out}} = 0.125$ on the outer mesh $\mathscr{T}_h \setminus (\mathscr{T}_h|_\omega)$. This yields 2542 elements and 703 nodes for $\mathscr{T}_h|_\omega$, as well as 23 434 elements and 4976 nodes for the overall mesh $\mathscr{T}_h$. The initial values $\boldsymbol{m}_h^0$ and $\boldsymbol{h}_h^0$ are obtained from relaxation with `FC-2` and $\boldsymbol{f} = 0$, of $\boldsymbol{m}^0 = (-1,-1,-1)/\sqrt{3}$, and $\boldsymbol{h}^0 = -\boldsymbol{m}^0$ on ω and $\boldsymbol{h}^0 = \boldsymbol{0}$ on $\overline{\Omega}\setminus\omega$. The exact solution is unknown. To compute the empirical convergence rates we consider a reference solution $\boldsymbol{m}_{hk_{\mathrm{ref}}}$ computed with `DC-2`, using the time-step size $k_{\mathrm{ref}} = 2^{-14}$.

Figure 4 visualizes the experimental convergence orders of the four integrators. As expected, the fully coupled approach `FC-2` and the decoupled approach `DC-2` lead to second-order convergence in time. As mentioned in Remark 3.1(v), `FC-1` and `DC-1` only lead to first-order convergence in time. Moreover, note that the decoupled approach `DC-2` is computationally as expensive as `DC-1`. In contrast to that, the fully coupled approach `FC-2` employs a fixed-point iteration at each time step and thus comes at the highest computational cost. Overall, the decoupled approach `DC-2` appears to be the method of choice with respect to both computational time and empirical accuracy.

Acknowledgements

The authors thank the anonymous referees for valuable comments that improved the algorithm considerably.

Funding

Austrian Science Fund (FWF) through the doctoral school *Dissipation and Dispersion in Nonlinear PDEs* (grant W1245); special research program *Taming Complexity in Partial Differential Systems* (grant SFB F65); Vienna Science and Technology Fund (WWTF) through the project *Thermally Controlled Magnetization Dynamics* (grant MA14-44).

References

Abert, C., Exl, L., Selke, G., Drews, A. & Schrefl, T. (2013) Numerical methods for the stray-field calculation: a comparison of recently developed algorithms. *J. Magn. Magn. Mater.*, **326**, 176–185.

Abert, C., Hrkac, G., Page, M., Praetorius, D., Ruggeri, M. & Suess, D. (2014) Spin-polarized transport in ferromagnetic multilayers: an unconditionally convergent FEM integrator. *Comput. Math. Appl.*, **68**, 639–654.

Alouges, F. (2008) A new finite element scheme for Landau–Lifchitz equations. *Discrete Contin. Dyn. Syst. Ser. S*, **1**, 187–196.

Alouges, F., Di Fratta, G. & Merlet, B. (2015) Liouville type results for local minimizers of the micromagnetic energy. *Calc. Var. Partial Differential Equations*, **53**, 525–560.

Alouges, F. & Jaisson, P. (2006) Convergence of a finite element discretization for the Landau–Lifshitz equation in micromagnetism. *Math. Models Methods Appl. Sci.*, **16**, 299–316.

Alouges, F., Kritsikis, E., Steiner, J. & Toussaint, J.-C. (2014) A convergent and precise finite element scheme for Landau–Lifschitz–Gilbert equation. *Numer. Math.*, **128**, 407–430.

Alouges, F., Kritsikis, E. & Toussaint, J.-C. (2012) A convergent finite element approximation for Landau–Lifschitz–Gilbert equation. *Physica B*, **407**, 1345–1349.

Alouges, F. & Soyeur, A. (1992) On global weak solutions for Landau–Lifshitz equations: existence and nonuniqueness. *Nonlinear Anal.*, **18**, 1071–1084.

Baibich, M. N., Broto, J. M., Fert, A., Van Dau, F. N., Petroff, F., Etienne, P., Creuzet, G., Friederich, A. & Chazelas, J. (1988) Giant magnetoresistance of (001)Fe/(001) Cr magnetic superlattices. *Phys. Rev. Lett.*, **61**, 2472–2475.

Baňas, L., Page, M. & Praetorius, D. (2015) A convergent linear finite element scheme for the Maxwell–Landau–Lifshitz–Gilbert equations. *Electron. Trans. Numer. Anal.*, **44**, 250–270.

Baňas, L., Page, M., Praetorius, D. & Rochat, J. (2014) A decoupled and unconditionally convergent linear FEM integrator for the Landau–Lifshitz–Gilbert equation with magnetostriction. *IMA J. Numer. Anal.*, **34**, 1361–1385.

Bartels, S. (2005) Stability and convergence of finite-element approximation schemes for harmonic maps. *SIAM J. Numer. Anal.*, **43**, 220–238.

Bartels, S. & Prohl, A. (2006) Convergence of an implicit finite element method for the Landau–Lifshitz–Gilbert equation. *SIAM J. Numer. Anal.*, **44**, 1405–1419.

Berger, L. (1996) Emission of spin waves by a magnetic multilayer traversed by a current. *Phys. Rev. B*, **54**, 9353–9358.

Bertotti, G., Magni, A., Mayergoyz, I. D. & Serpico, C. (2002) Landau–Lifshitz magnetization dynamics and eddy currents in metallic thin films. *J. Appl. Phys.*, **91**, 7559.

Binasch, G., Grünberg, P., Saurenbach, F. & Zinn, W. (1989) Enhanced magnetoresistance in layered magnetic structures with antiferromagnetic interlayer exchange. *Phys. Rev. B*, **39**, 4828–4830.

Bruckner, F., Feischl, M., Führer, T., Goldenits, P., Page, M., Praetorius, D., Ruggeri, M. & Suess, D. (2014) Multiscale modeling in micromagnetics: existence of solutions and numerical integration. *Math. Models Methods Appl. Sci.*, **24**, 2627–2662.

Cimrák, I. (2008) A survey on the numerics and computations for the Landau–Lifshitz equation of micromagnetism. *Arch. Comput. Methods Eng.*, **15**, 277–309.

Di Fratta, G., Pfeiler, C.-M., Praetorius, D., Ruggeri, M. & Stiftner, B. (2017) Linear second order IMEX-type integrator for the (eddy current) Landau–Lifshitz–Gilbert equation. *Extended preprint available at arXiv:1711.10715*.

Donahue, M. J. & Porter, D. G. (1999) OOMMF User's Guide, Version 1.0, *Interagency Report NISTIR 6376, National Institute of Standards and Technology*. MD: Gaithersburg.

Feischl, M. & Tran, T. (2017) The eddy current–LLG equations: FEM-BEM coupling and a priori error estimates. *SIAM J. Numer. Anal.*, **55**, 1786–1819.

Fredkin, D. R. & Koehler, T. R. (1990) Hybrid method for computing demagnetization fields. *IEEE Trans. Magn.*, **26**, 415–417.

García-Cervera, C. J. (2007) Numerical micromagnetics: a review. *Bol. Soc. Esp. Mat. Apl. SeMA*, **39**, 103–135.

Gilbert, T. L. (1955) A Lagrangian formulation of the gyromagnetic equation of the magnetization fields. *Phys. Rev.*, 100, 1243. Abstract only.

Hosomi, M., Yamagishi, H., Yamamoto, T., Bessho, K., Higo, Y., Yamane, K., Yamada, H., Shoji, M., Hachino, H., Fukumoto, C., Nagao, H. & Kano, H. (2005) A novel nonvolatile memory with spin torque transfer magnetization switching: Spin-RAM. *Proceedings of the IEEE International Electron Devices Meeting 2005. IEDM Technical Digest.*, IEEE. pp. 459–462.

Hrkac, G., Schrefl, T., Ertl, O., Suess, D., Kirschner, M., Dorfbauer, F. & Fidler, J. (2005) Influence of eddy current on magnetization processes in submicrometer permalloy structures. *IEEE Trans. Magn.*, **41**, 3097–3099.

Kružík, M. & Prohl, A. (2006) Recent developments in the modeling, analysis, and numerics of ferromagnetism. *SIAM Rev.*, **48**, 439–483.

Landau, L. & Lifshitz, E. (1935) On the theory of the dispersion of magnetic permeability in ferromagnetic bodies. *Phys. Zeitsch. der Sow.*, **8**, 153–168.

Le, K.-N., Page, M., Praetorius, D. & Tran, T. (2015) On a decoupled linear FEM integrator for eddy-current-LLG. *Appl. Anal.*, **94**, 1051–1067.

Le, K.-N. & Tran, T. (2013) A convergent finite element approximation for the quasi-static Maxwell–Landau–Lifshitz–Gilbert equations. *Comput. Math. Appl.*, **66**, 1389–1402.

Nédélec, J. C. (1986) A new family of mixed finite elements in QT. *Numer. Math*, **50**, 57–81.

NIST Micromagnetic Modeling Activity Group (2014). Available at https://www.ctcms.nist.gov/mumag/mumag.org.html.

Pfeiler, C.-M., Ruggeri, M., Stiftner, B., Exl, L., Hochsteger, M., Hrkac, G., Schöberl, J., Mauser, N. J. & Praetorius, D. (2019) Computational micromagnetics with Commics. *Comput. Phys. Commun.* doi: 10.1016/j.cpc.2019.106965. available online https://gitlab.asc.tuwien.ac.at/cpfeiler/commics.

Praetorius, D. (2004) Analysis of the operator Δ^{-1} div arising in magnetic models. *Z. Anal. Anwend*, **23**, 589–605.

Praetorius, D., Ruggeri, M. & Stiftner, B. (2018) Convergence of an implicit–explicit midpoint scheme for computational micromagnetics. *Comput. Math. Appl.*, **75**, 1719–1738.

Prohl, A. (2001) Computational micromagnetism. *Advances in Numerical Mathematics*. B. G. Vieweg+Teubner Verlag. Wiesbaden.

Quarteroni, A. & Valli, A. (1994) *Numerical Approximation of Partial Differential Equations*. Springer Series in Computational Mathematics, vol. 23. Springer. Berlin Heidelberg.

Schöberl, J. (2017). Netgen/NGSolve. Available at https://ngsolve.org/.

Slonczewski, J. C. (1996) Current-driven excitation of magnetic multilayers. *J. Magn. Magn. Mat.*, **159**, L1–L7.

Śmigaj, W., Betcke, T., Arridge, S., Phillips, J. & Schweiger, M. (2015) Solving boundary integral problems with BEM++. *ACM Trans. Math. Softw .*, **41**, 6:1–6:40.

Sun, J., Collino, F., Monk, P. B. & Wang, L. (2004) An eddy-current and micromagnetism model with applications to disk write heads. *Internat. J. Numer. Methods Engrg.*, **60**, 1673–1698.

Thiaville, A., Nakatani, Y., Miltat, J. & Suzuki, Y. (2005) Micromagnetic understanding of current-driven domain wall motion in patterned nanowires. *Europhys. Lett.*, **69**, 990–996.

Zhang, S. & Li, Z. (2004) Roles of nonequilibrium conduction electrons on the magnetization dynamics of ferromagnets. *Phys. Rev. Lett.*, **93**, 127204.